Theory of ion-temperature-gradient-driven turbulence in tokamaks

G. S. Lee, and P. H. Diamond

Citation: The Physics of Fluids **29**, 3291 (1986); doi: 10.1063/1.865846
View online: https://doi.org/10.1063/1.865846
View Table of Contents: https://aip.scitation.org/toc/pfl/29/10
Published by the American Institute of Physics

Theory of ion-temperature-gradient-driven turbulence in tokamaks

G. S. Lee and P. H. Diamond
Institute for Fusion Studies, The University of Texas at Austin, Austin, Texas 78712-1060

(Received 30 January 1986; accepted 15 July 1986)

An analytic theory of ion-temperature-gradient-driven turbulence in tokamaks is presented. Energy-conserving, renormalized spectrum equations are derived and solved in order to obtain the spectra of stationary ion-temperature-gradient-driven turbulence. Corrections to mixing-length estimates are calculated explicitly. The resulting anomalous ion thermal diffusivity $\chi_i = 0.4[(\pi/2)\ln(1+\eta_i)]^2[(1+\eta_i)/\tau]^2\rho_p^2 c_s/L_s$ is derived and is found to be consistent with experimentally deduced thermal diffusivities. The associated electron thermal and particle diffusivity, and particle and heat-pinch velocities are also calculated. The effect of impurity gradients on saturated ion-temperature-gradient-driven turbulence is discussed and a related explanation of density profile steepening during Z-mode operation is proposed.

I. INTRODUCTION

The search for an adequate understanding of energy confinement in tokamaks has motivated theoretical and experimental research in plasma physics for a long time. Most of this research effort has been oriented toward explaining observed anomalies in electron thermal energy confinement, while neoclassical transport theory has long been considered adequate for calculating ion thermal conduction. However, experimental results now suggest that significant anomalous ion thermal transport may also occur.

In particular, recent experiments on the Alcator-C tokamak[1,2] indicate that when the plasma density is large enough so that the electron–ion thermal equilibration time ($\tau_{ei} \sim 1/n^2$) approaches (from above) the neo-Alcator electron thermal energy confinement time ($\tau_{E_e} \sim n$), significant anomalous energy loss can occur through the ion conduction channel. The onset of this loss process occurs while τ_E begins to saturate. Furthermore, it was also observed that the injection of large pellets and the subsequent steepening of the plasma density gradient resulted in decreased ion thermal conduction. Electron enegy confinement remained in the neo-Alcator phase. This interesting result suggests that peaked density profiles may be favorable to reduced ion thermal conduction, and that an important relationship between particle and energy confinement exists, in general.

This trend appears to extend into auxiliary heating regimes, in spite of numerous complications in data analysis and interpretation. In particular, neutral beam injection (which directly heats ions) is nearly always accompanied by a degradation in overall energy confinement and a weakening of the density dependence of the energy confinement time τ_E, as it departs from that predicted by neo-Alcator Ohmic regime scaling. Furthermore, recent charge exchange recombination spectroscopy experiments on the D-III tokamak[3] during neutral beam injection have resulted in direct measurements of the magnitude and radial profile of the ion thermal conductivity $\chi_i(r)$. Substantial departures, in both magnitude and profile shape, from the neoclassical χ_i prediction are indicated. Finally, the observed density profile broadening, particle confinement time (τ_p) degradation, and density saturation (referred to as the "density clamp"), which frequently accompany the degradation of τ_E during cotangential injection, collectively reinforce the suspicion that ion thermal transport is closely linked to particle transport and confinement.

Ion-temperature-gradient-driven turbulence, which evolves from unstable ion-temperature-gradient modes (η_i modes, where $\eta_i = d\ln T_i/d\ln n$), has been proposed as a possible explanation of these results. Originally identified by Coppi *et al.*,[4] the ion-temperature-gradient instability is an electrostatic sound wave driven unstable by an ion-pressure gradient. For $\eta_i > \eta_{ic} \sim 1.5$, where η_{ic} denotes the critical value of η_i necessary for instability, the dynamics probably can be described using a simple fluid model where an adiabatic electron response is neutralized by an ion response determined by pressure ($\tilde{p}_i$), parallel velocity ($\tilde{v}_{\|i}$), and vorticity equations. A growth rate $\gamma \sim [(1+\eta_i)/\tau]^{1/2} k_y \rho_s c_s/L_s$, where L_s is the shear length, c_s is the sound speed, and ρ_s is the ion gyroradius at the electron thermal velocity, and a radial mode width $\lambda_r = [(1+\eta_i)/\tau]^{1/2}\rho_s$ are predicted. Approximate values of the pressure fluctuation level are $\tilde{p}_i/p_0 \sim \lambda_r/L_p$, where L_p is the ion pressure scale length, and the thermal diffusivity $\chi_i \sim [(1+\eta_i)/\tau]^{1/2}\rho_s^2 c_s/L_s$ can then be trivially deduced using familiar "mixing-length rules." The qualitative consistency of the predicted χ_i with experimentally determined ion thermal diffusivity values, the favorable scaling of χ_i with density gradient ($\eta_i \sim L_n/L_{T_i}$), and the simplicity and comparative parametric insensitivity of the plasma model collectively establish the ion-temperature-gradient mode as a very promising candidate for explaining anomalous ion thermal transport in tokamaks. Furthermore, extension of the simple electrostatic sheared slab model to include the effects of toroidicity, inductive electric fields, and nonadiabatic electron dynamics probably does not lead to conclusions which differ substantivally from those discussed above. Finally, it has been observed that ion-temperature-gradient instability may be enhanced by inverted impurity profiles and may drive an anomalous inward particle flow.[5]

A quantitative understanding of the experimental observations requires a theory of saturated ion-temperature-gradient-driven turbulence. The frequently invoked mixing-length "rules" (i.e., $\tilde{p}_i/p_0 \sim 1/k_x L_p$, $D \sim \gamma/k_x^2$) are neither

 0031-9171/86/103291-23$01.90

quantitatively accurate nor necessarily even qualitatively correct (i.e., see Ref. 6), and thus more careful analysis is required. Previous investigations of ion-temperature-gradient-driven turbulence gave been primarily devoted to such mixing-length estimates or simple extensions thereof. In particular, in Ref. 6 the anomalous ion thermal diffusivity and inward particle flow velocity were calculated using a mixing-length estimate ($e\tilde{\phi}/T_e \sim 1/k_x L_n$) of the electrostatic fluctuation level. However, both intuitive arguments and detailed theoretical analysis indicate that an estimate of the form $\tilde{p}_i/p_0 \sim 1/k_x L_p$ (i.e., pressure, rather than potential, "mixes") is more appropriate. Since $\tilde{p}_i/p_0 = \tilde{n}/n_0 + \tilde{T}_i/T_0 \neq e\tilde{\phi}/T_e$, the predictions of Ref. 7 differ, both qualitatively and quantitatively, from those presented here. The results of the first detailed nonlinear theory of ion-temperature-gradient-driven turbulence are discussed in Ref. 8. In that investigation, which dealt with a local model of the three-dimensional η_i mode system, a perturbation expansion was used to obtain mode-coupling equations. Solution of these equations yielded the saturation amplitude, which agreed with the simple mixing-length result. Several difficulties are apparent in this work. First, Eqs. (14)–(16) of Ref. 8 contain no dissipation effects, and thus cannot actually yield a stationary solution for $\eta_i > \eta_{ic}$. This difficulty is also manifested in the exact agreement of the mode-coupling result with the mixing-length estimate. In contrast, while the result of this investigation is similar to the mixing-length estimate, additional detailed functional dependencies, which are related to the nonlinear coupling of the fluctuations to the dissipative energy sink (ion Landau damping), also appear in the result. A second difficulty is the questionable treatment of incoherent mode coupling in Ref. 8. As a result, the consistency of the results with energy conservation constraints is dubious. Finally, it is worthwhile to note that the reason that none of the difficulties discussed here are manifested by the computational investigations described in Ref. 9 is because in that work, heating effects are omitted and the ion pressure gradient flattens. Thus, the results are representative of a quasilinear, rather than a nonlinear, saturation.

In this paper, a renormalized theory of ion-temperature-gradient-driven turbulence is presented. For $\eta_i > \eta_{ic}$, ion-temperature-gradient-driven turbulence is described by hydrodynamic equations for density, parallel velocity, and pressure

$$\frac{\partial n_i}{\partial t} + \nabla\cdot(n_i \mathbf{v}_{\perp i}) + \nabla_\parallel (n_i \tilde{v}_{\parallel i}) = 0,$$

$$m_i n_i \left(\frac{\partial \tilde{v}_{\parallel i}}{\partial t} + \mathbf{v}_E \cdot \nabla_\parallel \tilde{v}_{\parallel i}\right) = -e n_i \nabla_\parallel \Phi - \nabla_\parallel P_i + \mu_\parallel \nabla_\parallel^2 \tilde{v}_{\parallel i},$$

$$\frac{\partial P_i}{\partial t} + \tilde{v}_E \cdot \nabla P_i + \Gamma P_i \nabla_\parallel \tilde{v}_{\parallel i} = 0.$$

Three energy-like quadratic integrals

$$E^W = \frac{1}{2}\int d^3x(|\Phi|^2 + |\nabla_\perp \Phi|^2),$$

$$E^K = \frac{1}{2}\int d^3x|\tilde{v}_{\parallel i}|^2,$$

and

$$E^I = \frac{1}{2}\frac{1}{\Gamma}\int d^3x|\tilde{P}_i|^2,$$

which are useful in describing the nonlinear fluctuation dynamics, can be straightforwardly identified. The evolution of the fluctuation energies E^W, E^K, and E^I is governed by the two-point correlation equations

$$\frac{\partial}{\partial t}E^W = -\int d^3x[\Phi\nabla_\parallel \tilde{v}_{\parallel i} - \langle \Phi\hat{b}\times\nabla\Phi\cdot\nabla_\perp(\nabla_\perp^2\Phi)\rangle],$$

$$\frac{\partial}{\partial t}E^K = -\int d^3x[\tilde{v}_{\parallel i}\nabla_\parallel\Phi + \tilde{v}_{\parallel i}\nabla_\parallel\tilde{P}_i + \mu_\parallel\langle(\nabla_\parallel\tilde{v}_{\parallel i})^2\rangle + \langle\tilde{v}_{\parallel i}\hat{b}\times\nabla\Phi\cdot\nabla\tilde{v}_{\parallel i}\rangle],$$

$$\frac{\partial}{\partial t}E^I = -\int d^3x\left(\tilde{P}_i\nabla_\parallel\tilde{v}_{\parallel i} - \frac{1}{\Gamma}\langle\tilde{v}_r\tilde{P}_i\rangle\frac{d\langle P_0\rangle}{dr} + \frac{1}{\Gamma}\langle\tilde{P}_i\hat{b}\times\nabla\Phi\cdot\nabla\tilde{P}_i\rangle\right).$$

The various terms of the two-point correlation equations can be classified in three categories. The first, which includes the terms $\Phi\nabla_\parallel\tilde{v}_{\parallel i}$, $\tilde{v}_{\parallel i}\nabla_\parallel\tilde{P}_i$, and $\tilde{P}_i\nabla_\parallel\tilde{v}_{\parallel i}$, accounts for *linear* energy coupling (equipartitioning) due to sound wave propagation. The second category, which includes the terms

$$\langle\Phi\hat{b}\times\nabla\Phi\cdot\nabla_\perp(\nabla_\perp^2\Phi)\rangle, \quad \langle\tilde{v}_{\parallel i}\hat{b}\times\nabla\Phi\cdot\nabla\tilde{v}_{\parallel i}\rangle,$$

and $\langle\tilde{P}_i\hat{b}\times\nabla\Phi\cdot\nabla\tilde{P}_i\rangle$ is related to *nonlinear* energy transfer resulting from turbulent (c/B_0) $(\tilde{E}\times\hat{b})$ velocity shear stress. The third category includes the source term $(1/\Gamma)\langle\tilde{v}_i\tilde{P}_i\rangle d\langle P_0\rangle/dr$, proportional to the gradient of the average pressure, and the energy sink $-\mu_\parallel\langle(\nabla_\parallel\tilde{v}_{\parallel i})^2\rangle$, proportional to the parallel viscosity. Thus shear stress induced energy transfer nonlinearly couples the long wavelength energy sources with the short wavelength energy sink, resulting in saturated, stationary turbulence.

In order to quantitatively describe saturated ion-temperature-gradient-driven turbulence, it is necessary to construct and solve three coupled, renormalized (i.e., closed) energy spectrum evolution equations. In order to render this rather involved calculation analytically tractable, it is useful to identify the basic nonlinear spatial and temporal scales which characterize saturated ion-temperature-gradient-driven turbulence. The basic spatial scale (radial mixing-length) scale is $\Delta_{\mathbf{k}} = [D_{\mathbf{k}}/k'_\parallel]^{1/4}$, and is obtained by the asymptotic balance of the ion sound term with the vorticity convection term, where the $\tilde{E}\times\mathbf{B}$ nonlinearities have been renormalized $[(c/B_0)(\tilde{E}\times\hat{b})\cdot\nabla\rightarrow D_{\mathbf{k}}/\Delta_{\mathbf{k}}^2]$ and $D_{\mathbf{k}}$ refers to turbulent radial diffusion. The basic temporal scales are the nonlinear coherence (correlation) time

$$\tau_{c,\mathbf{k}} = \Delta\omega_{\mathbf{k}}^{-1} = [D_{\mathbf{k}}/\Delta_{\mathbf{k}}^2]^{-1},$$

the dissipation time

$$\tau_{d,\mathbf{k}} = \left(\mu_\parallel\int dx\,\frac{\langle(\nabla_\parallel\tilde{v}_\parallel)^2\rangle_{\mathbf{k}}}{E_{\mathbf{k}}^K}\right)^{-1},$$

and the energy equipartitioning time

$$\tau_{\mathrm{eq},\mathbf{k}} = \left(\int dx\,\frac{\langle\tilde{p}\nabla_\parallel\tilde{v}_\parallel\rangle_{\mathbf{k}}}{E_{\mathbf{k}}^I}\right)^{-1}.$$

In addition, it is useful to define a "Reynolds number" $\mathrm{Re}\equiv\tau_{d,\mathbf{k}}/\tau_{c,\mathbf{k}}$ which parametrizes the relative importance of

nonlinear decorrelation in comparison to dissipative processes. At saturation, the level of turbulence must be sufficient so that nonlinear transfer of fluctuation energy to dissipation balances fluctuation growth. Therefore,

$$\Delta\omega_{\mathbf{k}} \sim ([(1+\eta_i)/\tau]^2 k_\parallel' \Delta_{\mathbf{k}}^2/\Delta\omega_{\mathbf{k}}),$$

and

$$D_{\mathbf{k}} = [(1+\eta_i)/\tau]^{1/2} k_\parallel' \Delta_{\mathbf{k}}^3,$$

so that in turn

$$D_{\mathbf{k}} = [(1+\eta_i)/\tau]^2 (k_y\rho_s)\rho_s^2 c_s/L_s$$

and

$$\Delta_{\mathbf{k}} = [(1+\eta_i)/\tau]^{1/2}\rho_s.$$

Hence, the basic time scales are given by

$$\tau_{\mathrm{eq},\mathbf{k}}^{-1} = (\Gamma/\tau)[(1+\eta_i)/\tau](k_y\rho_s c_s/L_s),$$

$$\tau_{c,\mathbf{k}}^{-1} = [(1+\eta_i)/\tau](k_y\rho_s c_s/L_s),$$

and

$$\tau_{d,\mathbf{k}}^{-1} = [\mu_\parallel k_y^2/(k_{0x}^2 L_s^2)] \simeq (\tau)^{-1}(k_y\rho_s c_s/L_s),$$

so that $\tau_{\mathrm{eq},\mathbf{k}} < \tau_{c,\mathbf{k}} < \tau_{d,\mathbf{k}}$. The effective "Reynolds number" is given by

$$\mathrm{Re} = (k_{0x}^4 L_s^2 D_{\mathbf{k}}/\mu_\parallel k_{0y}^2) \simeq (1+\eta_i) \quad \text{for} \quad \eta_i > \chi_{ic}.$$

The problem of determining the saturation level of ion-temperature-gradient-driven turbulence can be simplified by exploiting the ordering $\tau_{\mathrm{eq},\mathbf{k}} < \tau_{c,\mathbf{k}} < \tau_{d,\mathbf{k}}$. In particular, $\tau_{\mathrm{eq},\mathbf{k}} < \tau_{c,\mathbf{k}}$ implies that energy "equipartitioning" among $E_{\mathbf{k}}^W$, $E_{\mathbf{k}}^K$, and $E_{\mathbf{k}}^I$ on a time scale faster than the nonlinear energy transfer time. Thus, $E_{\mathbf{k}}^W \simeq E_{\mathbf{k}}^K \simeq E_{\mathbf{k}}^I$, and the fluctuation energy evolution equations may be added yielding

$$\frac{\partial}{\partial t}\langle \mathscr{E}_{12}\rangle_{\mathbf{k}} + \langle S_{12}^I\rangle + T_{12} = \langle S_{12}^0\rangle,$$

where $\langle \mathscr{E}_{12}\rangle_{\mathbf{k}}$ refers to the total fluctuation energy for the mode $\mathbf{k}$. The $\langle \mathscr{E}_{12}\rangle_{\mathbf{k}}$ equation states that the fluctuation energy in mode $\mathbf{k}$ is determined by the balance of energy input due to pressure gradient relaxation

$$\langle S_{12}^0\rangle = \left(\frac{1}{\Gamma}\right)\langle \tilde{P}_i(2)\nabla_{y1}\tilde{\phi}(1)\rangle \frac{d\langle P_0\rangle}{dr} + \langle 1\leftrightarrow 2\rangle$$

with the nonlinear transfer

$$T_{12} = \langle \hat{b}\times\nabla_1\tilde{\phi}(1)\cdot\nabla_1\tilde{v}(1)\tilde{v}(2)\rangle + (1/\Gamma)\langle \hat{b}\times\nabla_1\tilde{\phi}(1)\cdot\nabla_1\tilde{P}_i(1)\tilde{P}_i(2)\rangle + \langle 1\leftrightarrow 2\rangle$$

of energy to viscous dissipation($\mu_\parallel\nabla_\parallel^2$). The fluctuation spectrum can then be obtained by solution of the $\langle \mathscr{E}_{12}\rangle_{\mathbf{k}}$ equation. In particular, for $k \gg k_0$, $\mathrm{Re} \gg 1$, $\langle \mathscr{E}_{12}\rangle_{\mathbf{k}} \sim k_y^{-5/2}$. The spectrum is cut off at the dissipation range wavenumber $k_d = \sqrt{\mathrm{Re}}\, k_{0y}$, where the spectrum averaged poloidal wavenumber $k_{0y}\rho_s = 0.4$ is obtained from the calculated spectrum.

Once the fluctuation spectrum has been determined, it is straightforward to calculate the ion thermal diffusivity and other transport coefficients. In particular,

$$\chi_i = [C(\mathrm{Re})]^2[(1+\eta_i)/\tau]^2(k_{0y}\rho_s)(\rho_s^2 c_s/L_s),$$

where $C(\mathrm{Re}) \simeq (\pi/2)\ln(1+\eta_i)$ and $k_{0y}\rho_s \simeq 0.4$. It is interesting to note that $\chi_i = F(\mathrm{Re})\chi_i^{\text{mixing-length}}$ so that the thermal diffusivity is given by the mixing-length estimate multiplied by a dimensionless function of the Reynolds number, determined from the calculated fluctuation spectrum. This functional form is characteristic of large Reynolds turbulence. Note that no undetermined parameters remain in the expression for χ_i. Finally, other transport coefficients can be calculated in a similar fashion.

In this paper, the theory of ion-temperature-gradient-driven turbulence is presented. The principal results are as follows.

(i) The fluctuation energy correlation function and fluctuation wavenumber spectra are calculated by solution of energy-conserving mode-coupling equations. The calculated wavenumber spectrum of ion pressure fluctuations has the form $\langle \tilde{P}_i^2\rangle_{k_\theta} \sim k_\theta^{-5/2}$, where

$$(\tilde{P}_i/P_{0i})_{\mathrm{rms}} \simeq 5.7[(1+\eta_i)/\tau]^{3/2}\rho_s/L_n.$$

Similarly, the rms fluctuating radial velocity is

$$(\tilde{v}_r)_{\mathrm{rms}} \simeq 2.3[(1+\eta_i)/\tau]^{3/2}\rho_s c_s/L_s$$

and fluctuating density is

$$(\tilde{n}/n_0) = (e\Phi/T_e) \simeq 5.7[(1+\eta_i)/\tau]^{3/2}\rho_s/L_s.$$

Note that the predicted density fluctuation levels are quite similar to the usual drift-wave turbulence level $\tilde{n}/n_0 \simeq 3\rho_s/L_n$. Hence, it may be difficult to experimentally distinguish η_i-mode induced density fluctuations from more commonplace low-frequency, drift-wave turbulence unless propagation direction (i.e., ion versus electron) can be resolved. While the parameter scalings of these results are qualitatively consistent with mixing-length estimates, they have been derived using the calculated fluctuation spectra. In particular, no assumptions such as $k_y\rho_s \sim \mathscr{O}(1)$, etc. were used to obtain the numerical coefficients.

(ii) For $\eta_i > \eta_{ic}$, the ion thermal diffusivity χ_i is given by

$$\chi_i = [C(\mathrm{Re})]^2[(1+\eta_i)/\tau]^2(k_{0y}\rho_s)(\rho_s^2 c_s/L_s),$$

where $C(\mathrm{Re}) \simeq (\pi/2)\ln(1+\eta_i)$. The numerical value of the ion thermal diffusivity is consistent with the experimentally measured χ_i for the Alcator-C tokamak (for which $k_{0y}\rho_s \simeq 0.4$). Furtherfore, for Alcator-C parameters $|C(\mathrm{Re})|^2 \cong 5$, which indicates the importance of the two-point theory in deriving quantitative predictions for comparision with experiment.

(iii) For dissipative trapped electron dynamics (i.e., $\nu_* < 1, \nu_{\mathrm{eff}} > \bar{\omega}_{De}$), the electron heat conductivity due to ion-temperature-gradient-driven turbulence is given by

$$\chi_e \simeq 15\sqrt{2}\epsilon^{3/2}\left(\frac{\pi}{2}\ln(1+\eta_i)\right)^4\left(\frac{1+\eta_i}{\tau}\right)^3 \frac{c_s^2\rho_s^2}{\nu_e L_s^2}(k_{0y}^2\rho_s^2).$$

Here ϵ is the inverse aspect ratio. Note that in general, $\chi_e \neq \chi_i$ and that χ_e is not determined by considerations of profile consistency.

(iv) For collisional electron dynamics (i.e., $k_\parallel v_{\mathrm{th},e} < \nu_{ie}$), the electron response to the ion-temperature-gradient-driven turbulence results in a particle flux:

$$\Gamma_r \simeq 2n_0[C(\mathrm{Re})]^4[\hat{\chi}_e + (1+\alpha_T)^2]\left(1-\frac{\eta_e}{\eta_e^c}\right)$$
$$\times\left(\frac{m_e}{m_i}\right)\frac{0.51}{\hat{\chi}_e}\frac{\nu_e}{L_n}\left(\frac{1+\eta_i}{\tau}\right)^2\rho_s^2,$$

where

$$\eta_e^c \simeq \left[\frac{\hat{\chi}_e + (1+\alpha_T)^2}{\frac{3}{2}(1+\alpha_T)}\right] \simeq 1.77.$$

Note that for $\eta_e > 1.77$, the flux is inward. For an Alcator-C parameter, $\langle V_r \rangle = \Gamma_r/n_0 \simeq 1000$ cm/sec. Similarly, the electron thermal flux Q_r^e can be derived. For $\eta_e > 2.65$, the electron thermal flux is inward and corresponds to a "heat-pinch." However, for *collisionless* electron dynamics, the particle flux is always outward. In particular, for $\nu_* < 1$,

$$\Gamma_r \cong n_0 \epsilon^{3/2}\left(\frac{\omega_{*e}(1+\frac{3}{2}\eta_e) - \mathrm{Re}(\omega)}{\nu_{ei}}\right)$$
$$\times\left(\frac{\pi^2}{4}[\ln(1+\eta_i)]^2\right)^2\left(\frac{1+\eta_i}{\tau}\right)^3\frac{(k_y\rho_s)_{\mathrm{rms}}\rho_s^2 c_s}{L_s^2}.$$

Hence, Γ_r *decreases* with η_i, thus reconciling energy and particle confinement time behavior during pellet injection experiments.

(v) The effects of impurity gradients on ion-temperature-gradient-driven turbulence have been investigated. For impurity density n_{0I} with scale length L_{nI}, $\chi_i \to \chi_i \Lambda^2$, and $\Gamma_r \to \Gamma_r \Lambda^3$, where $\Lambda = [1 + Z(n_{0I}/n_{0i})\,(L_{ni}/L_{nI})]^{-1}$. Thus impurity distributions peaked on axis heal η_i-mode turbulence while distributions peaked at the edge enhance it. In particular, the enhancement of Γ_r may underlie the density profile steepening observed during the Z mode of the ISX-B tokamak.

After the completion and presentation[10] of the results of this investigation, an alternative derivation of χ_i for ion-temperature-gradient-driven turbulence was proposed by Connor.[11] In that work, based on dimensional analysis of the ion fluid equations, a χ_i similar to that obtained using mixing-length rules was derived. Several difficulties are apparent in this work. First, no dissipation effects (such as $\mu_\parallel$) are included in the basic equations, which consequently do not even possess a stationary solution. Second, the dimensional analysis is actually performed on approximate ion fluid equations that omit parallel compressibility effects and thus do not conserve energy. Finally, as a consequence of the first difficulty, the χ_i actually derived has *no* functional dependence on $\mu_\parallel$ or Reynolds number. Such dependence must be present in a theory that correctly accounts for the energy sink and dissipation range (at large k_y) of the fluctuation spectrum. It is also worthwhile to note that the mixing-length rule predictions are, in general, too small to explain experimental results. This further strengthens the case for a detailed understanding of the fluctuation spectrum and its impact on transport.

The remainder of this paper is organized as follows. In Sec. II, the basic model and linear theory of the ion-temperature-gradient mode is reviewed. in Sec. III, a heuristic description of η_i mode turbulence is developed using mixing-length theory based on one-point renormalized equations. The renormalized two-point equation for the fluctuation energy correlation function is then derived. The energy mode-coupling equation is solved using a spatial representation technique, and the wavenumber spectrum is calculated. In Sec. IV, the detailed predictions of the theory for η_i mode turbulence in tokamaks are presented. The ion and electron thermal diffusivities, anomalous particle fluxes, and impurity effects are discussed. Section V includes the summary and conclusions.

II. BASIC MODEL AND LINEAR THEORY

An all-inclusive description of the ion-temperature-gradient-driven instability (η_i mode) requires the use of kinetic theory to treat the detailed linear properties such as threshold values of η_i, associated with ion–wave interaction (Landau damping), and finite Larmor radius corrections.[4,12] However, a comparison of the Vlasov dispersion relation with the dispersion relation obtained from fluid equations suggests that the fluid model adequately describes the essential physics of η_i mode in the phase velocity regime $v_{\mathrm{th},i} \lesssim |\omega/k_\parallel| < v_{\mathrm{th},e}$. That is, while fluid equations may obscure certain details of the linear stability theory and are not applicable to the case of flat density profile ($\eta_i > L_s/L_T$), they adequately describe the nonlinear dynamics in the range $\eta_{ic} < \eta_i < L_s/L_T$. Hence, the use of a fluid model is justified for parameter regimes appropriate to the confinement region of most tokamak plasmas.

Here, we derive the fluid equations to describe the evolution of the ion-temperature-gradient-driven turbulence. To simplify the analysis and construct an analytically tractable model of the nonlinear evolution of the η_i mode, we consider a simple radially inhomogeneous sheared slab of plasma. The magnetic field is given by $\mathbf{B} = B(\hat{z} + (x/L_s)\hat{y})$, where $L_s^{-1} = B_y'(x)/B_0$ is the shear length. The parallel wavenumber thus varies with x and is given by

$$k_\parallel(x) \simeq (x - x_{\mathbf{k}})\,(k_y/L_s), \tag{1}$$

in the neighborhood of the mode-rational surface $x_{\mathbf{k}}$, where $\mathbf{k}\cdot\mathbf{B}(x_{\mathbf{k}}) = 0$. In this geometry, low-frequency ($\omega \ll \omega_{ci}$) perturbations have the form

$$\tilde{f}(x)\exp(-i\omega t + ik_y y + ik_\parallel z).$$

To describe ion dynamics, the basic fluid model consists of the coupled equations for the ion density $\tilde{n}_i(\mathbf{x},t)$, parallel ion velocity $\tilde{v}_{\parallel i}(\mathbf{x},t)$, and ion pressure $\tilde{P}_i(\mathbf{x},t)$.[13] Quasineutrality with adiabatic electron response ($\tilde{n}_e = \tilde{n}_i = e\tilde{\Phi}/T_e$, since $|\omega/k_\parallel| \ll v_{\mathrm{th},e}$) and electrostatic dynamics are assumed. Thus, the continuity equation for the ion density is given by

$$\frac{\partial n_i}{\partial t} + \nabla\cdot(n_i \mathbf{v}_{\perp i}) + \nabla_\parallel(n_i \tilde{v}_{\parallel i}) = 0. \tag{2}$$

The perpendicular ion dynamics are due to $\mathbf{E}\times\mathbf{B}$ and ion diamagnetic drifts, so that to the first order in $\mathcal{O}(\omega/\omega_{ci})$:

$$\mathbf{v}_{\perp i,1} = \mathbf{v}_E + \mathbf{v}_{Di}, \tag{3}$$

where

$$\mathbf{v}_E = (c/B)\hat{b}\times\nabla\Phi$$

and

$$\mathbf{v}_{Di} = (c/eBn_i)\hat{b} \times \nabla P_i,$$

with

$$\hat{b} = \mathbf{B}/|\mathbf{B}|.$$

To the next order, the generalized ion polarization drift is given by

$$\mathbf{v}_p = -\frac{c^2 m_i}{eB^2}\left(\frac{\partial}{\partial t} + \mathbf{v}_{\perp,1} \cdot \nabla_\perp\right)\nabla_\perp \Phi.$$

Similarly, the equation of parallel motion is given by

$$m_i n_i \left(\frac{\partial \tilde{v}_{\parallel i}}{\partial t} + \mathbf{v}_E \cdot \nabla\, \tilde{v}_{\parallel i}\right) = -en_i \nabla_\parallel \Phi - \nabla_\parallel \tilde{P}_i + \mu_\parallel \nabla_\parallel^2 \tilde{v}_{\parallel i}. \tag{4}$$

It is important to note that the parallel flow is advected only by $\mathbf{v}_E$.[14] In Eq. (4) the parallel ion viscous diffusion term is retained. The parallel viscosity term models either collisionless Landau damping ($\mu_\parallel \sim v_{\text{th},i}^2/|\omega|$) or collisional parallel viscosity ($\mu_\parallel \sim v_{\text{th},i}^2/\nu_{ii}$). This parallel viscosity is a sink of energy in the large-k (i.e., dissipation) region of the wave-number spectrum and is especially important in the nonlinear theory. Finally, the evolution equation for ion pressure is

$$\frac{\partial P_i}{\partial t} + \mathbf{v}_E \cdot \nabla P_i + \Gamma P_i \nabla_\parallel \tilde{v}_{\parallel i} = 0, \tag{5}$$

where Γ is the ratio of the specific heats. The adiabatic compression term $\Gamma \nabla_\parallel \tilde{v}_{\parallel i}$, must be retained to account for energy exchange between pressure fluctuations and parallel velocity fluctuations in the nonlinear theory. However, this term has little effect on linear stability and the basic scales associated with the η_i modes.

To exploit the basic spatial and temporal scales characteristic of ion-drift modes (i.e., sound speed c_s and $\rho_s = c_s/\omega_{ci}$), we introduce a dimensionless form of the evolution equations where spatial scales are in units of ρ_s and the temporal scales are in units of ω_{ci}^{-1}. The dimensionless fields are defined in terms of the natural units of the average electron temperature T_e, the sound speed c_s, and the average ion pressure P_{i0}, so that the electrostatic potential is $\tilde{\phi} \equiv e\Phi/T_e$, the parallel ion momentum is $\tilde{v}_\parallel \equiv \tilde{v}_{\parallel i}/c_s$, and the ion pressure is $\tilde{p} \equiv [\tilde{p}_i/\langle P_{i0}\rangle](T_i/T_e)$, where $P_i = \langle P_{i0}\rangle + \tilde{p}_i$ and $n_i = n_0 + \tilde{n}_i$. We thus obtain the basic set of fluid equations, which describes ion-temperature-gradient-driven turbulence from Eqs. (2)–(5), which yield

$$\frac{\partial}{\partial t}(1 - \nabla_\perp^2)\tilde{\phi} + v_D\left[1 + \left(\frac{1+\eta_i}{\tau}\right)\nabla_\perp^2\right]\nabla_y \tilde{\phi} - \hat{b} \times \nabla\tilde{\phi} \cdot \nabla_\perp(\nabla_\perp^2 \tilde{\phi}) + \nabla_\parallel \tilde{v}_\parallel = 0, \tag{6}$$

$$\frac{\partial}{\partial t}\tilde{v}_\parallel + \hat{b} \times \nabla\tilde{\phi} \cdot \nabla\tilde{v}_\parallel - \mu\nabla_\parallel^2 \tilde{v}_\parallel = -\nabla_\parallel \tilde{\phi} - \nabla_\parallel \tilde{p}, \tag{7}$$

$$\frac{\partial}{\partial t}\tilde{p} + v_D\left(\frac{1+\eta_i}{\tau}\right)\nabla_y \tilde{\phi} + \hat{b} \times \nabla\tilde{\phi} \cdot \nabla\tilde{p} = -\Upsilon \nabla_\parallel \tilde{v}_\parallel, \tag{8}$$

where

$$v_D \equiv -\frac{cT_e}{eB}\frac{d(\ln n_0)}{dx}, \quad \tau \equiv \frac{T_e}{T_i}, \quad \eta_i = \frac{d(\ln T_i)}{d(\ln n_0)},$$

$$\Upsilon \equiv \frac{\Gamma}{\tau}, \quad \mu \equiv \frac{\mu_\parallel \omega_{ci}}{c_s^2}.$$

In writing Eqs. (6)–(8), we retain only the dominant nonlinearities due to $\mathbf{E}\times\mathbf{B}$ convection. In order to understand the nonlinear dynamics of ion-temperature-gradient-driven turbulence, it is essential to consider the energetics of the system. The energy flows and energy balance can be elucidated by consideration of energy-like integrals quadratic in the fluctuating field amplitudes. These energy-like integrals are defined by the sum of the electrostatic energy (electron internal energy) and (ion) perpendicular kinetic energy

$$E^W \equiv \frac{1}{2}\int d^3x(|\tilde{\phi}|^2 + |\nabla_\perp \tilde{\phi}|^2), \tag{9}$$

the parallel ion kinetic energy

$$E^K \equiv \frac{1}{2}\int d^3x|\tilde{v}_\parallel|^2, \tag{10}$$

and the ion thermal energy

$$E^I \equiv \frac{1}{2}\frac{1}{\Upsilon}\int d^3x|\tilde{p}|^2. \tag{11}$$

Using the evolution equations for density, ion parallel velocity, and ion pressure, these energy-like integrals can readily be shown to satisfy certain relations by use of the conservation property of convective nonlinearities (i.e., $\int d^3x \tilde{A}\nabla\tilde{\phi} \times \hat{b} \cdot \nabla\tilde{A} = 0$ for any $\tilde{A}$). It follows that

$$\frac{\partial}{\partial t}E^W = -\int d^3x\, \tilde{\phi}\nabla_\parallel \tilde{v}_\parallel, \tag{12}$$

$$\frac{\partial}{\partial t}E^K = -\int d^3x(\tilde{v}_\parallel \nabla_\parallel \tilde{\phi} + \tilde{v}_\parallel \nabla_\parallel \tilde{p} + \mu|\nabla_\parallel \tilde{v}_\parallel|^2), \tag{13}$$

$$\frac{\partial}{\partial t}E^I = -\int d^3x\left[\tilde{p}\nabla_\parallel \tilde{v}_\parallel + \frac{1}{\Upsilon}\left(\frac{1+\eta_i}{\tau}\right)v_D\langle \tilde{p}\nabla_y\tilde{\phi}\rangle\right]. \tag{14}$$

Hence, the total energy of the system evolves according to

$$\frac{\partial}{\partial t}E = -\int d^3x\left[\frac{1}{\Upsilon}\left(\frac{1+\eta_i}{\tau}\right)v_D\langle \tilde{p}\nabla_y\tilde{\phi}\rangle + \mu|\nabla_\parallel \tilde{v}_\parallel|^2\right]. \tag{15}$$

These evolution equations state that the coupling terms $\tilde{\phi}\nabla_\parallel \tilde{v}_\parallel$ and $\tilde{p}\nabla_\parallel \tilde{v}_\parallel$ account for transfer of fluctuation energy between fields. Hence, the sum is conserved up to the difference of drive by ion-temperature-gradient source and dissipation by ion parallel viscous diffusion. In the saturated state, nonlinear processes dynamically regulate the balance of input from the ion-temperature-gradient free-energy source with the linear dissipation due to parallel viscosity $\mu_\parallel$ (sink). Naturally, a stationarity of total energy evolution is a necessary condition for saturation.

The linear theory of the ion-temperature-gradient-driven stability has been investigated by many authors,[4,7,8,12,15] using both kinetic and fluid models in slab and toroidal geometry. Here, we do not attempt to address all details, nor undertake a review of the linear theories. However, it is instructive to review aspects of the linear theory from the viewpoint of developing a nonlinear theory. Within the framework of our model equations, the linear eigenmode equation can be derived in a straightforward manner by assuming a space-time variation of the form

$$\tilde{f}(x)\exp\left[-i\omega t + i\int k_x(x)dx + ik_y y\right]$$

and $k_\perp \rho_s < 1$, so that we obtain the eigenmode equation

$$\frac{d^2}{dx^2}\tilde{\phi}_{\mathbf{k}} + Q(x,\Omega)\tilde{\phi}_{\mathbf{k}} = 0, \tag{16}$$

where the potential function is given by

$$Q(x,\Omega) = \left(-k_y^2 + \frac{[1-\Omega]}{(\Omega + [(1+\eta_i)/\tau])} + \frac{(L_n/L_s)^2 x^2}{\Omega^2[1-(\Gamma/\tau)(L_n/L_s)^2 x^2/\Omega^2]}\right) \tag{17}$$

with

$$\Omega \equiv \omega/\omega_{*e} = \omega/(k_y v_D).$$

From this linear eigenmode equation, we can determine basic spatial and temporal scales of the η_i mode such as the mode width, the growth rate, and the real frequency. In Eq. (16), we neglect the effects associated with Landau damping and finite Larmor radius corrections. This is appropriate for the fluid ion regime which describes the low-$k_\perp$ region of the wavenumber spectrum. This is an especially good model for high-shear regions of tokamak plasmas (i.e., $\hat{s} = rq'/q \gtrsim 1$), where toroidicity corrections are probably insignificant.

The WKB eigenvalue condition for the Weber equation gives the following dispersion relation:

$$\Omega^2(1+k_y^2) + \Omega\left[k_y^2\left(\frac{1+\eta_i}{\tau}\right) + i(2n+1)\frac{L_n}{L_s} - 1\right] + i(2n+1)\frac{(1+\eta_i)}{\tau}\frac{L_n}{L_s} = 0, \tag{18}$$

where $n = 0,1,...$ are radial wavenumbers. For small wavenumbers, $k_y^2 \ll [\tau/(1+\eta_i)] < 1$, the growth rate and mode width for the unstable ion-drift mode are given by $\Omega \simeq i(1+\eta_i/\tau)L_n/L_s$ and $\lambda_r \simeq [(1+\eta_i)/\tau]^{1/2}$, respectively. It is important to notice that the η_i mode in this wavenumber regime is almost purely growing, with growth rate scaling inversely with the shear length. For the wavenumber regime of $k_y^2 \simeq [\tau/(1+\eta_i)] < 1$, the restoring force along **B** is stronger and the η_i mode has a real frequency comparable to the growth rate. The complex eigenfrequency is given by

$$\Omega = \omega_r + i\gamma \simeq \left(\frac{-1+i}{\sqrt{2}}\right)\left(\frac{[(1+\eta_i)/\tau]L_n/L_s}{(1+k_y^2)}\right)^{1/2}.$$

The mode width does not vary significantly from the value for smaller k_y, provided the inequality $|\gamma| > |\omega_r|$ is satisfied. Throughout the range of wavenumbers (i.e., $k_y^2 \simeq [\tau/(1+\eta_i)] < 1$), the potential-well structure is found to persist, and the growth rate is larger than the real frequency.

Detailed numerical (shooting code) solutions of the linear eigenmode equation, including kinetic effects, have been obtained by Waltz *et al.*[16] These numerical studies indicate that the most unstable mode is located in the low-k_y region of the wavenumber spectrum ($k_y^2 < 1$) and the effective potential in this regime is found to be a well structure that can be adequately described by the potential function of Eq. (17). Hence, the eigenfunction has the character of a radially localized normal mode (Fig. 1). These unstable modes are the principal free-energy source for the turbulence. For higher-k_y ($k_y^2 \gtrsim 1$), ω_r/γ progressively increases and exceeds unity. The potential-well structure disappears and turns into a potential hill. Hence, the eigenmode takes on the character of a propagating wave (Fig. 2). The wave energy is then susceptible to absorption by shear damping, which results in parallel ion heating at the large-$k_\parallel$ region of the eigenmode. The higher-k_y damped modes are a sink of fluctuation energy. Hence, a possible saturation mechanism is nonlinear energy transfer from low-k_y unstable modes into the high-k_y damped modes. In order to incorporate the important stabilizing effect associated with shear damping into the fluid theory, the sink of fluctuation energy is modeled by a parallel ion viscosity with coefficient $\mu_\parallel$, which represents the damping of the high-k_y modes. It should be noted that the effect of the parallel viscosity on the low-k_y modes is weak, and the detailed nonlinear study shows that the saturated state has a weak dependence upon the value of the viscosity coefficient $\mu_\parallel$ within the range of η_i values where the fluid theory is applicable.

Finally, it is necessary to point out that for the two limiting cases associated with $\eta_i \sim \eta_{ic}$ and flat density, the fluid ion approximation is not valid. These two limiting cases have been previously discussed in studies of linear stability[7,15] and we will not repeat the results in this paper. However, it should be noted that the range of η_i values where the fluid theory is applicable ($\eta_{ic} < \eta_i < L_s/L_T$) seems to correspond to most parameter regimes of experimental interest.[10]

III. NONLINEAR THEORY

In this section, the analytical theory of the nonlinear evolution and saturation of ion-temperature-gradient-driven turbulence is presented. The fluctuation levels, spectra,

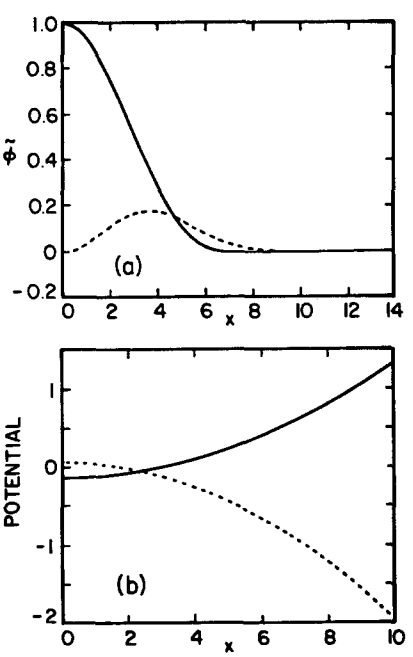

FIG. 1. Complex eigenmode (a), and potential function (b) for $k_y\rho_s = 0.3$, $\eta_i = 4$, $T_e/T_i = 1$, and $L_n/L_s = 1/20$.

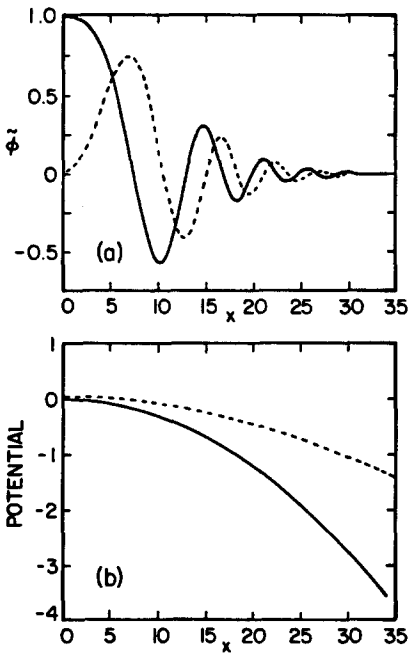

FIG. 2. Complex eigenmode (a), and potential function (b) for $k_y\rho_s = 0.7$, $\eta_i = 4$, $T_e/T_i = 1$, and $L_n/L_s = 1/20$.

and the thermal diffusivity at saturation are calculated. The implications of these results for predictions of heat and particle transport in tokamak plasma are then discussed in Sec. IV.

Before proceeding with our discussions of the dynamics of nonlinear evolution and saturation of ion-temperature-gradient-driven turbulence, we pause to consider the question of whether quasilinear flattening of the average ion-temperature gradient or turbulent stabilization via nonlinear coupling to dissipation is the relevant saturation mechanism. In the case of η_i-mode turbulence in tokamaks, the average ion-temperature gradient is driven by the balance of power input, through Ohmic and neutral beam heating, with thermal transport. Furthermore, the density profile is determined by particle transport dynamics. Thus the η_i profile is determined by external drive. Although η_i-mode-induced heat loss can be substantial, it is not catastrophic, since predicted χ_i values are consistent with experimental observations. As marginal stability scenarios usually are based on the notion that violation of the marginal stability condition results in catastrophic transport (i.e., much larger than that actually observed), an *a priori* assertion that the η_i profile is determined by marginal stability considerations seems unreasonable. Thus, quasilinear mechanisms alone are not adequate for the description of η_i-mode saturation, and nonlinear mechanisms must be considered.

The organization of this section is as follows: we begin with a heuristic description of η_i-mode turbulence using renormalized one-point theory and mixing-length estimates to outline the physics of the saturation mechanism and the energy dynamics of the system. We identify the important basic temporal and spatial scales and the Reynolds number of the η_i-mode system, and estimate the level of fluctuations and the thermal diffusion coefficient at saturation. We proceed to develop a more detailed nonlinear theory, utilizing a spatial representation of the two-point spectral energy equation to quantitatively calculate the wavenumber spectrum and the fluctuation level. Finally, a brief review of the nonlinear theory and a summary of results are presented.

A. Heuristic description

Nonlinear theories based on heuristic ambient-gradient or mixing-length estimates (i.e., $|e\Phi/T_e| \sim 1/k_\perp L_{T_i}$, $D \sim \gamma/k_\perp^2$) do not necessarily account for the dynamics of nonlinear evolution and saturation of η_i-mode turbulence. Furthermore, since the mode width is a function of the linear growth rate, the meaning of the mixing-length estimate of saturation is unclear when growth rates vanish. Thus, it is necessary to determine spatial and temporal scales associated with saturated η_i-mode turbulence. Also, it is necessary to derive and solve a spectrum equation that properly accounts for energy flow from source to sink via nonlinear coupling.

Now, we consider the nonlinear evolution of η_i-mode turbulence using the equations derived previously. This set of nonlinear equations can be analyzed by renormalizing the nonlinearities using iterative substitution techniques, and considering the nonlinear evolution of a linearly unstable η_i mode in a background spectrum of multiple-helicity turbulence. The relevant nonlinear spatial and temporal scales can thus be identified. Renormalized two-point equations are then used to calculate the fluctuation levels and spectra.

Fourier transforming Eqs. (6)–(8) in the y and z directions, the nonlinear evolution equations for the test mode (k) can be written as

$$\frac{\partial}{\partial t}(1-\nabla_\perp^2)\tilde{\phi}_{\mathbf{k}} + i\left(1+\frac{(1+\eta_i)}{\tau}\nabla_\perp^2\right)\omega_{*e}\tilde{\phi}_{\mathbf{k}} + ik_\parallel \tilde{v}_{\parallel\mathbf{k}}$$
$$+\left\{\left[\frac{\partial}{\partial x}\left(\sum_{\mathbf{k}'}(-ik_y')\tilde{\phi}_{-\mathbf{k}'}\nabla_\perp^2\tilde{\phi}_{\mathbf{k}''}\right)\right.\right.$$
$$\left.-ik_y\sum_{\mathbf{k}'}\frac{\partial\tilde{\phi}_{-\mathbf{k}'}}{\partial x'}\nabla_\perp^2\tilde{\phi}_{\mathbf{k}''}\right]$$
$$-\left[\frac{\partial}{\partial x}\left(\sum_{\mathbf{k}'}(-ik_y')\,(\nabla_\perp^2\tilde{\phi}_{-\mathbf{k}'})\tilde{\phi}_{\mathbf{k}''}\right)\right.$$
$$\left.\left.-ik_y\sum_{\mathbf{k}'}\frac{\partial(\nabla_\perp^2\tilde{\phi}_{-\mathbf{k}'})}{\partial x'}\tilde{\phi}_{\mathbf{k}''}\right]\right\} = 0, \tag{19}$$

$$\frac{\partial}{\partial t}\tilde{v}_{\parallel\mathbf{k}} + ik_\parallel\tilde{\phi}_{\mathbf{k}} + ik_\parallel\tilde{p}_{\mathbf{k}} + \mu k_\parallel^2\tilde{v}_{\parallel\mathbf{k}}$$
$$-\left\{\left[\frac{\partial}{\partial x}\left(\sum_{\mathbf{k}'}(-ik_y')\tilde{\phi}_{-\mathbf{k}'}\tilde{v}_{\parallel\mathbf{k}''}\right) - ik_y\sum_{\mathbf{k}'}\frac{\partial\tilde{\phi}_{-\mathbf{k}'}}{\partial x'}\tilde{v}_{\parallel\mathbf{k}''}\right]\right.$$
$$\left.-\left[\frac{\partial}{\partial x}\left(\sum_{\mathbf{k}'}(-ik_y^2)\tilde{v}_{\parallel-\mathbf{k}'}\tilde{\phi}_{\mathbf{k}''}\right) - ik_y\sum_{\mathbf{k}'}\frac{\partial\tilde{v}_{\parallel-\mathbf{k}'}}{\partial x'}\tilde{\phi}_{\mathbf{k}''}\right]\right\}$$
$$= 0, \tag{20}$$

$$\frac{\partial}{\partial t}\tilde{p}_{\mathbf{k}} + i\frac{(1+\eta_i)}{\tau}\omega_{*e}\tilde{\phi}_{\mathbf{k}} + ik_{\parallel}\Upsilon\tilde{v}_{\parallel\mathbf{k}} - \left\{\left[\frac{\partial}{\partial x}\left(\sum_{\mathbf{k}'}(-ik_y')\tilde{\phi}_{-\mathbf{k}'}\tilde{p}_{\mathbf{k}''}\right) - ik_y\sum_{\mathbf{k}'}\frac{\partial\tilde{\phi}_{-\mathbf{k}'}}{\partial x'}\tilde{p}_{\mathbf{k}''}\right] - \left[\frac{\partial}{\partial x}\left(\sum_{\mathbf{k}'}(-ik_y')\tilde{p}_{-\mathbf{k}'}\tilde{\phi}_{\mathbf{k}''}\right) - ik_y\sum_{\mathbf{k}'}\frac{\partial\tilde{p}_{-\mathbf{k}'}}{\partial x'}\tilde{\phi}_{\mathbf{k}''}\right]\right\} = 0, \tag{21}$$

where $\mathbf{k} = (k_y, k_z)$, and the "driven" mode is $\mathbf{k}'' = \mathbf{k} + \mathbf{k}'$ with $\mathbf{k}'$ as the "background" mode and $\mathbf{k}$ as the "test" mode. To obtain renormalized equations, a standard weak coupling closure approximation[17] is used to renormalize the (convective) nonlinearities by iteratively substituting the nonlinearly driven fields $\tilde{\phi}^{(2)}_{\mathbf{k}''}$, $(\nabla_\perp^2\tilde{\phi}_{\mathbf{k}''})^{(2)}$, $\tilde{v}^{(2)}_{\parallel\mathbf{k}''}$, and $\tilde{p}^{(2)}_{\mathbf{k}''}$ for $\tilde{\phi}_{\mathbf{k}''}$, $\nabla^2_{\perp\mathbf{k}''}$, $\tilde{v}_{\mathbf{k}''}$, and $\tilde{p}_{\mathbf{k}''}$, respectively. Here $\tilde{\phi}^{(2)}_{\mathbf{k}''}$, $(\nabla_\perp^2\tilde{\phi}_{\mathbf{k}''})^{(2)}$, $\tilde{v}^{(2)}_{\parallel\mathbf{k}''}$, and $\tilde{p}^{(2)}_{\mathbf{k}''}$ are nonlinearly driven by the direct beating of the test ($\mathbf{k}$) and background ($\mathbf{k}'$) modes. These driven fields satisfy the equations

$$\Delta\omega_{\mathbf{k}''}(1-\nabla_\perp^2)\tilde{\phi}^{(2)}_{\mathbf{k}''} + i\omega''_{*e}\{1+[(1+\eta_i)/\tau]\nabla_\perp^2\}\tilde{\phi}^{(2)}_{\mathbf{k}''} + ik''_{\parallel}\tilde{v}^{(2)}_{\parallel\mathbf{k}''} = S_\phi, \tag{22}$$

$$\Delta\omega_{\mathbf{k}''}\tilde{v}^{(2)}_{\parallel\mathbf{k}''} + ik''_{\parallel}\tilde{\phi}^{(2)}_{\mathbf{k}''} + ik''_{\parallel}\tilde{p}^{(2)}_{\mathbf{k}''} = S_v, \tag{23}$$

$$\Delta\omega_{\mathbf{k}''}\tilde{p}^{(2)}_{\mathbf{k}''} + i[(1+\eta_i)/\tau]\omega''_{*e}\tilde{\phi}^{(2)}_{\mathbf{k}''} + ik''_{\parallel}\Upsilon\tilde{v}^{(2)}_{\parallel\mathbf{k}''} = S_p, \tag{24}$$

where S_ϕ, S_v, and S_p are the sources for the driven mode ($\mathbf{k}''$) and are given by

$$S_\phi = \left(ik_y'\tilde{\phi}_{\mathbf{k}'}\frac{\partial}{\partial x}(\nabla_\perp^2\tilde{\phi}_{\mathbf{k}}) - ik_y\frac{\partial\tilde{\phi}_{\mathbf{k}'}}{\partial x'}(\nabla_\perp^2\tilde{\phi}_{\mathbf{k}}) + ik_y\tilde{\phi}_{\mathbf{k}}\frac{\partial}{\partial x'}(\nabla_\perp^2\tilde{\phi}_{\mathbf{k}'}) - ik_y'\frac{\partial\tilde{\phi}_{\mathbf{k}}}{\partial x}(\nabla_\perp^2\tilde{\phi}_{\mathbf{k}'})\right), \tag{25}$$

$$S_v = \left(ik_y'\tilde{\phi}_{\mathbf{k}'}\frac{\partial\tilde{v}_{\parallel\mathbf{k}}}{\partial x} - ik_y\frac{\partial\tilde{\phi}_{\mathbf{k}'}}{\partial x'}\tilde{v}_{\parallel\mathbf{k}} + ik_y\tilde{\phi}_{\mathbf{k}}\frac{\partial\tilde{v}_{\parallel\mathbf{k}'}}{\partial x'} - ik_y'\frac{\partial\tilde{\phi}_{\mathbf{k}}}{\partial x}\tilde{v}_{\parallel\mathbf{k}'}\right), \tag{26}$$

$$S_p = \left(ik_y'\tilde{\phi}_{\mathbf{k}'}\frac{\partial\tilde{p}_{\mathbf{k}}}{\partial x} - ik_y\frac{\partial\tilde{\phi}_{\mathbf{k}'}}{\partial x'}\tilde{p}_{\mathbf{k}} + ik_y\tilde{\phi}_{\mathbf{k}}\frac{\partial\tilde{p}_{\mathbf{k}'}}{\partial x'} - ik_y'\frac{\partial\tilde{\phi}_{\mathbf{k}}}{\partial x}\tilde{p}_{\mathbf{k}'}\right). \tag{27}$$

Here, $\Delta\omega_{\mathbf{k}''}$ is the decorrelation rate for test ($\mathbf{k}$) and background ($\mathbf{k}'$) modes, and thus serves to limit the time scale of nonlinear interaction. The solutions of the driven mode equations can be obtained by convolving an integral transformation of the source functions with the global propagator for the field $\tilde{\phi}_{\mathbf{k}}$. However, a simple, approximate solution is sufficient to understand the basic dynamics of the nonlinear processes which we intend to discuss in this section. In particular, the turbulence is characterized by a single radial scale. Thus, the large-x asymptotic balance which determines the effective radial scale is dominated by the direct term contributions and, for this purpose, the $\tilde{\phi}^{(2)}_{\mathbf{k}''}$ terms (which contribute integral operators) can be ignored. With these approximations, driven fields are given approximately by

$$(\nabla_\perp^2\tilde{\phi}_{\mathbf{k}''})^{(2)} \simeq S_\phi/[\Delta\omega_{\mathbf{k}''}], \tag{28}$$

$$\tilde{v}^{(2)}_{\parallel\mathbf{k}''} \simeq S_v/[\Delta\omega_{\mathbf{k}''}], \tag{29}$$

$$\tilde{p}^{(2)}_{\mathbf{k}''} \simeq S_p/[\omega_{\mathbf{k}''}]. \tag{30}$$

Note that the neglect of $\tilde{\phi}^{(2)}_{\mathbf{k}''}$ is consistent with the conservation law symmetry properties of the $\tilde{v}_\parallel$, $\tilde{p}$ and $\langle\tilde{v}_\parallel^2\rangle$, $\langle\tilde{p}^2\rangle$ equations. The symmetry properties of the vorticity equation can be preserved by noting, for localized modes,

$$\frac{\partial}{\partial x}\sum_{\mathbf{k}'} -ik_y[\tilde{\phi}_{\mathbf{k}'}(\nabla_\perp^2\tilde{\phi}_{\mathbf{k}''}) - (\nabla_\perp^2\tilde{\phi}_{-\mathbf{k}'})\tilde{\phi}_{-\mathbf{k}''}] = \frac{\partial}{\partial x}\sum_{\mathbf{k}'}\left(-ik_y\frac{k_y^2}{k_y''^2}\right)[\tilde{\phi}_{-\mathbf{k}'}(\nabla_\perp^2\tilde{\phi}_{-\mathbf{k}''})],$$

where an integration by parts has been performed. Substituting the driven-field solutions into the nonlinear coupling terms in Eqs. (19)–(21) (noting the radial parity of the fields) yields the renormalized equations which govern the evolution of the test mode ($\mathbf{k}$):

$$\frac{\partial}{\partial t}(1-\nabla_\perp^2)\tilde{\phi}_{\mathbf{k}} + i\omega_{*e}\left(1+\frac{(1+\eta_i)}{\tau}\nabla_\perp^2\right)\tilde{\phi}_{\mathbf{k}} + \frac{\partial}{\partial x}\times\left(D_{\mathbf{k}}\frac{\partial}{\partial x}(\nabla_\perp^2\tilde{\phi}_{\mathbf{k}})\right) - C_{\mathbf{k}}k_y^2\tilde{\phi}_{\mathbf{k}} = -ik_{\parallel}\tilde{v}_{\parallel\mathbf{k}}, \tag{31}$$

$$\frac{\partial}{\partial t}\tilde{v}_{\parallel\mathbf{k}} - \frac{\partial}{\partial x}\left(D_{\mathbf{k}}\frac{\partial}{\partial x}\tilde{v}_{\parallel\mathbf{k}}\right) + C_{\mathbf{k}}k_y^2\tilde{v}_{\parallel\mathbf{k}} + \mu k_{\parallel}^2\tilde{v}_{\parallel\mathbf{k}} = -ik_{\parallel}\tilde{\phi}_{\mathbf{k}} - ik_{\parallel}\tilde{p}_{\mathbf{k}}, \tag{32}$$

$$\frac{\partial}{\partial t}\tilde{p}_{\mathbf{k}} - \frac{\partial}{\partial x}\left(D_{\mathbf{k}}\frac{\partial}{\partial x}\tilde{p}_{\mathbf{k}}\right) + C_{\mathbf{k}}k_y^2\tilde{p}_{\mathbf{k}} = -i\frac{(1+\eta_i)}{\tau}\omega_{*e}\tilde{\phi}_{\mathbf{k}} - ik_{\parallel}\Upsilon\tilde{v}_{\parallel\mathbf{k}}, \tag{33}$$

where

$$D_{\mathbf{k}} \equiv \sum_{\mathbf{k}'}\frac{(k_y')^2|\tilde{\phi}_{\mathbf{k}'}|^2}{\Delta\omega_{\mathbf{k}+\mathbf{k}'}},$$

and

$$C_{\mathbf{k}} \equiv \sum_{\mathbf{k}'}\frac{|\partial\tilde{\phi}_{\mathbf{k}'}/\partial x'|^2}{\Delta\omega_{\mathbf{k}+\mathbf{k}'}}.$$

Here, the diffusion coefficients $D_{\mathbf{k}}$ and $C_{\mathbf{k}}$ account for the principal nonlinear process, which is random convection of fluid elements by electrostatic turbulence. Note that only diffusive effects have been retained in the renormalized vorticity equation. This is because the diffusion terms dominate the large-x asymptotic balance, which in turn determines the basic scales of the turbulence. Obviously, more terms[18] must be retained in a complete, energy-conserving renormalization.

Having derived the renormalized equation for η_i-mode turbulence, we now discuss the saturation mechanism associated with turbulent damping of unstable sound-wave propagation and the general properties of the saturated state of η_i-mode turbulence in a simple heuristic manner. Since η_i-mode turbulence is a driven system with (linear) viscous dissipation damping the smallest scales, it is necessary to delineate the different spatial scales associated with "inertial" or "dissipation" ranges. Thus, it is necessary to parametrize the relative importance of $\mathbf{E}\times\mathbf{B}$ turbulent convection and linear viscous diffusion. Hence, it is useful to define, in the usual fashion, a Reynolds number as the ratio of the nonlinear term to the linear dissipation term in the dynami-

cal equation for $\tilde{v}_\parallel$. Thus, the Reynolds number for the η_i-mode system is defined by

$$\mathrm{Re} \equiv \frac{[D_{\mathbf{k}}/\Delta_{\mathbf{k}}^2]}{[\mu k_{0y}^2(\Delta_{\mathbf{k}}^2/L_s^2)]} = \frac{\tau_{d,\mathbf{k}}}{\tau_{c,\mathbf{k}}}, \tag{34}$$

where $\tau_{d,\mathbf{k}}$ refers to the linear dissipation time associated with ion parallel viscosity and $\tau_{c,\mathbf{k}}$ refers to the coherence time (eddy-turnover time) associated with nonlinear scrambling by $\mathbf{E}\times\mathbf{B}$ convection. Here, $\Delta_{\mathbf{k}}$ is the poloidal wavenumber dependent radial correlation length and k_{0y} is the rms poloidal wavevector. Upon estimation of $\Delta_{\mathbf{k}}$, to be discussed below, it follows that for long wavelengths $\mathrm{Re} \sim (1+\eta_i)$. Hence, this system has a finite width inertial range spectrum for the parameter regime of experimental interest. Here, inertial range means $\tau_c \ll \tau_d$, but allows for fluctuation growth due to η_i relaxation. Thus, our definition is different from that used in Navier–Stokes turbulence. Finally, note that the fluid model is especially well-suited for large Reynolds number regimes. For high Reynolds numbers, the basic picture of saturation is constructed and the basic nonlinear spatial and temporal scales can be obtained by using a mixing-length theory based on the assumption of maximal turbulent energy transfer, which ignores the details of the energy sink. This information is then used in a more complete and quantitative calculation of the fluctuation spectra. in particular such calculations properly account for the role of the dissipative energy sink in determining the saturation level of the turbulence.

To describe the saturated state, it is natural to specify the saturation condition as $\partial/\partial t(E^W + E^K + E^I) = 0$, namely that total fluctuation energy must be stationary in time. When this criterion is satisfied (ignoring localized quasilinear profile flattening) the energy evolution equations, Eqs. (12)–(15), state that drive by $d\langle P_{0i}\rangle/dx$ relaxation balances energy exchange (equipartitioning) by the linear coupling term $\tilde{\phi}\nabla_\parallel \tilde{v}_\parallel$, and that viscous parallel dissipation balances the sound-wave coupling destabilization term in Eq. (13). Then saturation can be achieved by energy flow from ion-temperature-gradient energy source to ion parallel dissipation, i.e.,

$$\mu \int d^3x |\nabla_\parallel \tilde{v}_\parallel|^2 = \frac{1}{\Upsilon}\int d^3x \langle \tilde{p}\nabla_y \tilde{\phi}\rangle \left(\frac{d\langle P_{0i}\rangle}{dx}\right).$$

This transfer is dynamically regulated by the nonlinear coupling and by the linear equipartitioning terms. That is, the unstable fluctuations are excited primarily at low-k_y (large scales) by tapping the ion-temperature-gradient free-energy source. Interactions among these large-scale unstable modes remove wave energy by transferring energy to smaller scales and ultimately to stable fluctuations. This nonlinear scrambling process is accounted for in the renormalized equations by turbulent diffusion. Therefore, for large Re, mixing-length theory based on maximal turbulent transfer can be used to qualitatively (but not quantitatively) describe the saturated state.

It is important to notice that the familiar Hasegawa–Mima[19] vorticity equation nonlinearity due to nonlinear polarization drift does not play as important a role in this case as in the quasi-two-dimensional case of drift-wave turbulence. This is because the η_i mode is fundamentally a three-dimensional sound wave with dynamics determined by the pressure and velocity field evolution. Indeed, in local theory the polarization drift can be ignored. Nonlocally, it serves primarily to set the radial eigenmode scale.

Setting the temporal derivative equal to zero and using the nonlinear radial scale $\Delta_{\mathbf{k}}$ from the renormalized ion pressure equation [Eq. (33)], we can relate the pressure response $\tilde{p}_{\mathbf{k}}$ to the electrostatic potential fluctuation $\tilde{\phi}_{\mathbf{k}}$ by asymptotically balancing turbulent $\mathbf{E}\times\mathbf{B}$ mixing of a localized pressure fluctuation over a nonlinear mode width with the ion-temperature-gradient driving term, thus obtaining

$$\tilde{p}_{\mathbf{k}} \simeq i[(1+\eta_i)/\tau](\omega_{*e}\tilde{\phi}_{\mathbf{k}}/\Delta\omega_{\mathbf{k}}), \tag{35}$$

where $\Delta\omega_{\mathbf{k}} = D_{\mathbf{k}}/\Delta_{\mathbf{k}}^2$ is the decorrelation rate associated with $\mathbf{E}\times\mathbf{B}$ turbulent convection. Substituting this relation into the ion parallel momentum balance equation [Eq. (32)], and balancing turbulent diffusion of ion parallel momentum (which couples to the destabilizing $\tilde{p}$ fluctuation) with the potential fluctuation, and then solving for $D_{\mathbf{k}}$ yields the diffusion rate required for mixing-length saturation. This diffusivity is given by

$$D_{\mathbf{k}} \simeq [(1+\eta_i)/\tau]^{1/2} k_\parallel' \Delta_{\mathbf{k}}^3, \tag{36}$$

where $k_\parallel' \equiv k_y/L_s$ in a sheared slab.

The dissipation mechanism for η_i-mode turbulence can be clearly seen by rewriting the ion parallel momentum balance equation using a heuristic balance argument as above. This yields

$$(\Delta\omega_{\mathbf{k}} + \mu k_\parallel^2 + (k_\parallel^2/\Delta\omega_{\mathbf{k}})[(1+\eta_i)/\tau])\tilde{v}_{\parallel\mathbf{k}} \simeq S_{\mathbf{k}}^0, \tag{37}$$

where the source of ion parallel momentum is given by $S_{\mathbf{k}}^0 \simeq \Upsilon(k_\parallel^2/\Delta\omega_{\mathbf{k}})\tilde{v}_{\parallel\mathbf{k}}$. This equation states that the ion parallel momentum fluctuation is driven by the transfer of pressure fluctuation energy, which taps the ion-temperature-gradient source through the compressional coupling term, and is dampled by turbulent $\mathbf{E}\times\mathbf{B}$ convection to parallel viscous dissipation. That is, for the most unstable low-k_y modes, the parallel viscosity due to ion Landau damping is too weak to stabilize the fluctuation, but draining of energy by a cascade process effectively couples to larger parallel viscosity at larger k_y. This in turn cuts off the unstable propagating sound waves and saturates the turbulence. It should be noted that although a mixing-length theory was used to estimate the level of diffusion in the saturated state in this heuristic section, the picture of saturation is different from that of previously proposed theories which either invoked naïve mixing-length rules or relied on an analogy to the Hasegawa–Mima-type nonlinear vorticity equation system to achieve saturation. Theories which are naive mixing-length rules to estimate the saturation amplitude of the fluctuations describe the process of saturation by turbulent mixing of a pressure fluctuation over a linear eigenmode within one linear growth time. The other theory[8] relies on an analogy to the Hasegawa–Mima equation in order to redistribute fluctuation energy throughout $k_\perp$ space by mode-coupling processes, thus coupling to perpendicular viscosity in higher-$k_\perp$ modes which are the ultimate sink of energy. A linear ion parallel momentum balance equation is assumed and hence

the important effect of turbulent transport of ion parallel momentum is neglected. These theories fail to discuss the important saturation mechanism associated with the cutoff of unstable sound-wave propagation by turbulent convection of ion parallel momentum to dissipation. They thus lead to spurious physical pictures of saturation which are not consistent with energy conservation or which do not include sound-wave dynamics or properly treat the effects of dissipation.

To complete our discussion of the saturated state, the nonlinear radial scale must be determined in order to estimate the diffusion coefficient. The nonlinear radial scale can be estimated from the continuity equation by balancing vorticity diffusion with destabilizing sound-wave coupling. Thus, the turbulent mixing-length scale is given by

$$\Delta_{\mathbf{k}} \simeq (D_{\mathbf{k}}/k_{\parallel}')^{1/4}. \tag{38}$$

Using the estimated diffusion level $D_{\mathbf{k}}$ in Eq. (36), which is necessary to maintain dynamical balance of turbulent transfer of energy with ion-temperature-gradient drive, it follows that saturation occurs for mixing lengths

$$\Delta_{\mathbf{k}} \simeq [(1+\eta_i)/\tau]^{1/2}, \tag{39}$$

with diffusion of the order of

$$D_{\mathbf{k}} \simeq [(1+\eta_i)/\tau]^2 (k_y/L_s). \tag{40}$$

A more quantitative calculation of diffusion level at saturation will be presented in the following discusison of the formal nonlinear theory. With these two conditions Eqs. (39) and (40), the nonlinear evolution of η_i modes can be described in the following way. Before reaching saturation, the spectrum gains energy from the ion-temperature-gradient free-energy source. The diffusion $D_{\mathbf{k}}$, and therefore the nonlinear radial scale $\Delta_{\mathbf{k}}$, increase. This process continues until energy drain by nonlinear coupling (of correlated diffusion) is sufficient to balance the driving force. A qualitative but not quantitative estimate of the fluctuation level at which this balance occurs is given by the mixing-length limit. At this point the perturbation is saturated and a stationary state is achieved.

Having elucidated the basic saturation mechanism and calculated the diffusion level at saturation, it is now possible to estimate a number of relevant quantities and scales that characterize saturated η_i-mode turbulence. These include the mean-square radial velocity, the rms value of potential fluctuations, and the level of pressure fluctuation, as well as the nonlinear coherence time, equipartitioning time and dissipation time scales. Using the definition of $D_{\mathbf{k}}$ and making a Markovian approximation (i.e., $\Delta\omega_{\mathbf{k}'}$ will replace $\Delta\omega_{\mathbf{k}+\mathbf{k}'}$ in the driven propagator), the level of diffusion at saturation, Eq. (40), can be rewritten as

$$D = \sum_{\mathbf{k}'} \frac{(k_y')^2 |\tilde{\phi}_{\mathbf{k}'}|^2}{\Delta\omega_{\mathbf{k}'}} = \sum_{\mathbf{k}'} \frac{E_{\mathbf{k}'}}{\Delta\omega_{\mathbf{k}'}} \simeq \left(\frac{1+\eta_i}{\tau}\right)^2 \frac{(k_y)_{\rm rms}}{L_s}, \tag{41}$$

where $E_{\mathbf{k}'} = (k_y')^2 |\tilde{\phi}_{\mathbf{k}'}|^2$ is the radial velocity squared. Then the rms radial velocity can be estimated as

$$(\tilde{v}_r)_{\rm rms} \simeq [(1+\eta_i)/\tau]^{3/2} [(k_y)_{\rm rms}/L_s], \tag{42}$$

and the rms value of the electrostatic potential fluctuation level is

$$(\tilde{n})_{\rm rms} = (\tilde{\phi})_{\rm rms} \simeq [(1+\eta_i)/\tau]^{3/2} (1/L_s).$$

In a similar fashion, the rms value of pressure fluctuation level can be estimated by using the stationary relation of $\tilde{p}$ and $\tilde{\phi}$ at saturation. It follows that

$$(\tilde{p})_{\rm rms} \simeq [(1+\eta_i)/\tau]^{3/2} (1/L_s).$$

Because of the $(k_y)_{\rm rms}$ dependence in various estimated quantities, it is necessary to calculate $(k_y)_{\rm rms}$ at saturation. This is possible only with the knowledge of the spectrum of fluctuations. Hence, we will calculate this value after the spectrum calculation, presented in the next section.

In addition to the quantities estimated above, the basic temporal scales associated with the nonlinear processes are also important, in order to address questions of energy flow. First of all, the basic nonlinear scrambling time can be defined by the eddy-turnover time associated with $\mathbf{E}\times\mathbf{B}$ turbulent convection, and is given by

$$\tau_{c,\mathbf{k}}^{-1} \equiv [D_{\mathbf{k}}/\Delta_k^2] \simeq [(1+\eta_i)/\tau](k_y/L_s).$$

Second, the dissipation time can be defined by using ion Landau damping as an effective parallel dissipation mechanism (here, $\mu \simeq v_{{\rm th},i}^2/|\omega|$ models the parallel viscosity caused by ion Landau damping), and is given by

$$\tau_{d,\mathbf{k}}^{-1} \equiv \frac{\mu \int dx \langle |\nabla_{\parallel} \tilde{v}_{\parallel}|^2 \rangle_{\mathbf{k}}}{E_{\mathbf{k}}^K} \simeq \left(\frac{k_y}{\tau L_s}\right).$$

Note here $\Delta_{\mathbf{k}}$ is used for x in $k_{\parallel}$. Recall that using these two time scales, the Reynolds number for η_i-mode turbulence (defined previously) can be estimated to be

$$\mathrm{Re} \equiv \tau_{d,\mathbf{k}}/\tau_{c,\mathbf{k}} \simeq (1+\eta_i)$$

when η_i must be large enough to use the fluid model. It is also important to define the equipartitioning time between $E_{\mathbf{k}}^W$, $E_{\mathbf{k}}^K$, and $E_{\mathbf{k}}^I$ through the linear energy exchange process,

$$\tau_{\mathrm{eq},\mathbf{k}}^{-1} \equiv (\int dx \langle \tilde{p} \nabla_{\parallel} \tilde{v}_{\parallel} \rangle_{\mathbf{k}})/E_{\mathbf{k}}^I$$

By using the stationarity relation, the equipartitioning time can be estimated as

$$\tau_{\mathrm{eq},\mathbf{k}}^{-1} \simeq \Upsilon [(1+\eta_i)/\tau](k_y/L_s).$$

For the large but finite value of η_i, it is important to notice that the hierarchy of these time scales is given by

$$\tau_{\mathrm{eq}} \lesssim \tau_c < \tau_d.$$

The importance of this hierarchy will be addressed in the following section.

B. Formal nonlinear theory

In the preceding section, the dynamics of the saturated state have been discussed, and fluctuation saturation levels and the basic scales associated with ion-temperature-gradient-driven turbulence have been estimated using one-point renormalized equations. Although this information is important for a basic physical understanding of η_i-mode turbulence and the resulting confinement scaling of tokamak experiments, a quantitative description of the wavenumber

spectrum of the fluctuations requires construction and solution of energy spectra evolution equations. For example, the average wavenumber $(k_y)_{\rm rms}$ cannot be determined from one-point theory and can be obtained only by use of energy spectrum equations.

Before considering the dynamics of energy evolution, it is necessary to discuss energy conservation and energy flow in wavenumber space. The wavenumber space evolution equations for the energy-like integrals (with triplets renormalized) are given by

$$\frac{\partial}{\partial t}E^W = -\sum_{\mathbf{k}}\int dx\,\tilde{\phi}_{-\mathbf{k}}k_\parallel\tilde{v}_{\parallel\mathbf{k}} + \sum_{\mathbf{k}}\int dx\Bigg(\sum_{\mathbf{k}'}\frac{(k_y')^2|\tilde{\phi}_{\mathbf{k}'}|^2}{\Delta\omega_{\mathbf{k}'}}\left\langle\frac{\partial\tilde{\phi}_{-\mathbf{k}}}{\partial x}\cdot\frac{\partial}{\partial x}(\nabla_1^2\tilde{\phi}_{\mathbf{k}})\right\rangle - \sum_{\mathbf{k}'}\frac{\langle(\partial\tilde{\phi}_{-\mathbf{k}'}/\partial x')\cdot(\partial/\partial x')\,(\nabla_1^2\tilde{\phi}_{\mathbf{k}'})\rangle}{\Delta\omega_{\mathbf{k}'}}k_y^2|\tilde{\phi}_{\mathbf{k}}|^2\Bigg), \tag{43}$$

$$\frac{\partial}{\partial t}E^K = -i\sum_{\mathbf{k}}\int dx(\tilde{v}_{\parallel-\mathbf{k}}k_\parallel\tilde{\phi}_{\mathbf{k}} + \tilde{v}_{\parallel-\mathbf{k}}k_\parallel\tilde{p}_{\mathbf{k}}) - \mu\sum_{\mathbf{k}}\int dx\,k_\parallel^2\langle\tilde{v}_{\parallel-\mathbf{k}}\tilde{v}_{\parallel\mathbf{k}}\rangle - \sum_{\mathbf{k}}\int dx\Bigg(\sum_{\mathbf{k}'}\frac{(k_y')^2|\tilde{\phi}_{\mathbf{k}'}|^2}{\Delta\omega_{\mathbf{k}'}}\left|\frac{\partial\tilde{v}_{\parallel\mathbf{k}}}{\partial x}\right|^2 + \sum_{\mathbf{k}'}\frac{|\partial\tilde{\phi}_{\mathbf{k}'}/\partial x'|^2}{\Delta\omega_{\mathbf{k}'}}k_y^2|\tilde{v}_{\parallel\mathbf{k}}|^2\Bigg) + \sum_{\mathbf{k}}\int dx\sum_{\mathbf{p}+\mathbf{q}=\mathbf{k}}\Bigg(\frac{p_y^2|\tilde{\phi}_{\mathbf{q}}|^2}{\Delta\omega_{-\mathbf{p}-\mathbf{q}}}\left|\frac{\partial\tilde{v}_{\parallel\mathbf{q}}}{\partial x}\right|^2 + \frac{q_y^2|\partial\tilde{\phi}_{\mathbf{p}}/\partial x|^2}{\Delta\omega_{-\mathbf{p}-\mathbf{q}}}|\tilde{v}_{\parallel\mathbf{q}}|^2\Bigg), \tag{44}$$

$$\frac{\partial}{\partial t}E^I = -i\sum_{\mathbf{k}}\int dx\,\tilde{p}_{-\mathbf{k}}k_\parallel\tilde{v}_{\parallel\mathbf{k}} + \frac{i}{\Upsilon}\sum_{\mathbf{k}}\int dx\langle\tilde{p}_{-\mathbf{k}}k_y\tilde{\phi}_{\mathbf{k}}\rangle\left(\frac{d\langle P_{0i}\rangle}{dx}\right) - \frac{1}{\Upsilon}\sum_{\mathbf{k}}\int dx\Bigg(\sum_{\mathbf{k}'}\frac{(k_y')^2|\tilde{\phi}_{\mathbf{k}'}|^2}{\Delta\omega_{\mathbf{k}'}}\left|\frac{\partial\tilde{p}_{\mathbf{k}}}{\partial x}\right|^2 + \sum_{\mathbf{k}'}\frac{|\partial\tilde{\phi}_{\mathbf{k}'}/\partial x'|^2}{\Delta\omega_{\mathbf{k}'}}k_y^2|\tilde{p}_{\mathbf{k}}|^2\Bigg) + \frac{1}{\Upsilon}\sum_{\mathbf{k}}\int dx\sum_{\mathbf{p}+\mathbf{q}=\mathbf{k}}\Bigg(\frac{p_y^2|\tilde{\phi}_{\mathbf{p}}|^2}{\Delta\omega_{-\mathbf{p}-\mathbf{q}}}\left|\frac{\partial\tilde{p}_{\mathbf{k}}}{\partial x}\right|^2 + \frac{q_y^2|\partial\tilde{\phi}_{\mathbf{p}}/\partial x|^2}{\Delta\omega_{-\mathbf{p}-\mathbf{q}}}|\tilde{p}_{\mathbf{q}}|^2\Bigg). \tag{45}$$

In Sec. II, we discussed energy flow and conservation of energy in configuration space, and identified compressional and sound-wave coupling terms that transfer energy between fields. In mixing-length theory, saturation of low-k_y modes (for $\mathrm{Re}>1$) can be estimated by invoking turbulent mixing, represented as a diffusion process, as a vehicle for draining energy from the low-k_y modes. Since the one-point theory does not conserve energy, saturation levels can at best be qualitatively estimated using mixing-length theory. However, spectral energy equations conserve energy. Thus, they are the natural tool for a spectrum calculation consistent with the basic conservation properties of the system.

Except for the vorticity nonlinearity, the renormalized convective nonlinearities have the common structure that the coherent part of the turbulent response drains energy, and the incoherent part refurnishes energy by emission. This competition results in an energy cascade. We can also identify an energy transfer mechanism from source to sink by noting the role of the compressional coupling term. The coupling term, $\int dx\,\tilde{p}\nabla_\parallel\tilde{v}_\parallel$, transfers pressure fluctuation energy to parallel momentum fluctuation energy through equipartitioning. Hence, ion-temperature-gradient-driven internal energy in $\langle\tilde{p}^2\rangle$ can be transferred to parallel kinetic energy in $\langle\tilde{v}_\parallel^2\rangle$ and ultimately dissipated through parallel viscosity at the high-k sink. It should also be noted that the hierarchy of time scales associated with these important processes (i.e., $\tau_{\rm eq}<\tau_c\ll\tau_d$) shows that equipartitioning can take place on a nonlinear time scale that is shorter than a correlation time and much shorter than a dissipation time. Even though equipartitioning takes place among all three fields $\tilde{\phi}$, $\tilde{v}_\parallel$, and $\tilde{p}$, the most important dynamics of energy flow are controlled by the evolution of $\langle\tilde{p}^2\rangle$ and $\langle\tilde{v}_\parallel^2\rangle$, which couple directly to the energy source and sink.

With these observations, a theory of energy evolution can be constructed by assuming equipartitioning of energy and by absorbing E^W into a total kinetic energy. The dynamics of nonlinear energy evolution can be described by two-point, one-time energy spectrum equations for $\langle\tilde{p}^2\rangle$ and $\langle\tilde{v}^2\rangle$, which retain incoherent emission as well as coherent diffusion. Here, the $\langle\tilde{v}^2\rangle$ term represents the total kinetic energy from E^W and E^K. Two-point equations for the energy spectrum can be obtained straightforwardly from the one-point equations, Eqs. (6)–(8), by multiplying by the field at a second point and taking an ensemble average. After symmetrizing, the resulting equations are

$$\frac{\partial}{\partial t}\langle\tilde{v}(1)\tilde{v}(2)\rangle - \mu(\nabla_{\parallel1}^2+\nabla_{\parallel2}^2)\langle\tilde{v}(1)\tilde{v}(2)\rangle + T_{12}^v = -\langle\tilde{v}(2)\nabla_{\parallel1}\tilde{p}(1)\rangle - \langle\tilde{v}(1)\nabla_{\parallel2}\tilde{p}(2)\rangle, \tag{46}$$

$$\frac{1}{\Upsilon}\frac{\partial}{\partial t}\langle\tilde{p}(1)\tilde{p}(2)\rangle + T_{12}^p = -\langle\tilde{p}(2)\nabla_{\parallel1}\tilde{v}(1)\rangle - \langle\tilde{p}(1)\nabla_{\parallel2}\tilde{v}(2)\rangle + \frac{1}{\Upsilon}[\langle\tilde{p}(2)\nabla_{y1}\tilde{\phi}(1)\rangle + \langle\tilde{p}(1)\nabla_{y2}\tilde{\phi}(2)\rangle]\left(\frac{d\langle P_{0i}\rangle}{dx}\right), \tag{47}$$

where T^v_{12} and T^p_{12} are triplets due to convective nonlinearities. The triplets are given by

$$T^v_{12} = \langle \hat{b} \times \nabla_1 \tilde{\phi}(1) \cdot \nabla_1 \tilde{v}(1) \tilde{v}(2) \rangle + \langle 1 \leftrightarrow 2 \rangle, \tag{48}$$

$$T^p_{12} = (1/\Upsilon) \langle \hat{b} \times \nabla_1 \tilde{\phi}(1) \cdot \nabla_1 \tilde{p}(1) \tilde{p}(2) \rangle + \langle 1 \leftrightarrow 2 \rangle. \tag{49}$$

Here, the slow time-scale variations are described by the time derivative, and $\langle 1 \leftrightarrow 2 \rangle$ stands for term with indices 1 and 2 exchanged. The evolution equation for the total energy can be obtained by adding two equations and assuming equipartition of energy between fields. This resulting equation can be formally written as

$$\frac{\partial}{\partial t} \langle \mathscr{E}_{12} \rangle + \langle S^I_{12} \rangle + T_{12} = \langle S^0_{12} \rangle, \tag{50}$$

where

$$\langle \mathscr{E}_{12} \rangle \equiv \langle \tilde{v}(1) \tilde{v}(2) \rangle + (1/\Upsilon) \langle \tilde{p}(1) \tilde{p}(2) \rangle$$

represents the total energy correlation function,

$$\langle S^0_{12} \rangle \equiv \frac{1}{\Upsilon} \langle \tilde{p}(2) \nabla_{y1} \tilde{\phi}(1) \rangle \left(\frac{d \langle P_{0i} \rangle}{dx} \right) + \langle 1 \leftrightarrow 2 \rangle$$

is the fluctuation source, proportional to the ion-temperature gradient,

$$\langle S^I_{12} \rangle \simeq -\mu (\nabla^2_{\|1} + \nabla^2_{\|2}) \langle \tilde{v}(1) \tilde{v}(2) \rangle$$

is the sink, representing dissipation by parallel viscosity, and

$$T_{12} \equiv T^v_{12} + T^p_{12}$$

is the nonlinearity (mode coupling). Here, it is important to notice that the nonlinearities (triplets) vanish as the relative separation goes to zero, while the source and sink do not. Turbulent mixing, which is represented by the transfer term, destroys all but the smallest spatial scales (smaller than the spatial correlation scale) on the time scale of a correlation time. Also note that the gradient source drives energy at all scales, and that the dissipative effects of parallel viscosity are also included in this system. Unlike the turbulent mixing process, these produce diffusion that stays finite as the relative separation goes to zero. This scale-independent decay mechanism destroys small-scale correlation in the "dissipation" region of spectrum where dissipation effects dominates nonlinear processes. Hence, this two-point energy evolution equation incorporates the basic effects of dissipation, source, and turbulent transfer.

While the neglect of incoherent mode coupling (an approximation made in the one-point theory) does not significantly alter the predicted fluctuation levels and scalings, the spectrum is sensitive to the effects of incoherent mode coupling. Hence, for the large Reynolds regime case considered here, the steady-state two-point correlation is determined not by the balance of ion-temperature-gradient drive with parallel viscous dissipation, but by inhomogeneities in the transfer terms associated with mode coupling. In order to analytically solve the spectral energy equation, here we use a spatial representation, which is an application of the methods of renormalized two-point theory (clump theory) to this fluid plasma system. The basic techniques utilized were originally proposed in the context of phase space density turbulence.[20] In this case, transfer in wavenumber space is represented by spatially inhomogeneous relative diffusion. By inverting the spatially represented energy evolution operator, the structure of the wavenumber spectrum can be obtained. This inversion accounts for the spatially inhomogeneous turbulent scattering process, as well as the coupling to the dissipation and turbulent diffusion which determines the decay of the correlation. This procedure enables us to obtain an analytic solution of the mode-coupling equation. Furthermore, the inversion of the operator determines the spectrum balance (steady-state) condition which in turn determines the saturation level.

Now, we can find the evolution operator in the spatial representation.[18] We transform the evolution equation for the two-point (energy) correlation, Eq. (50), to a relative coordinate system $(\mathbf{x}_+, \mathbf{x}_-)$, where $\mathbf{x}_+ = \frac{1}{2}(\mathbf{x}_1 + \mathbf{x}_2)$ is the average position of the points 1 and 2, and $\mathbf{x}_- = \frac{1}{2}(\mathbf{x}_1 - \mathbf{x}_2)$ is the relative position between them. Here, it is necessary to renormalize the nonlinearities (triplets), which describe turbulent scattering of energy due to temporally and spatially varying potential fluctuations. The weak coupling closure with standard iteration scheme used in the previous section is used to renormalize the triplets. Introducing Fourier expansions in the y and z directions, the triplets can be written as

$$\begin{aligned} T_{12} = \sum_{\mathbf{k}} \sum_{\mathbf{k}'} \sum_{\mathbf{k}''} \Big\langle & \exp(ik_y y_1 + ik_z z_1) \exp(ik'_y y_1 + ik'_z z_1) \exp(ik''_y y_2 + ik''_z z_2) \\ & \times \Big[\Big(-ik_y \tilde{\phi}_{\mathbf{k}}(1) \frac{\partial \tilde{v}_{\mathbf{k}'}}{\partial x_1}(1) \tilde{v}_{\mathbf{k}''}(2) + ik'_y \frac{\partial \tilde{\phi}_{\mathbf{k}}}{\partial x_1}(1) \tilde{v}_{\mathbf{k}'}(1) \tilde{v}_{\mathbf{k}''}(2) \Big) \\ & + \frac{1}{\Upsilon} \Big(-ik_y \tilde{\phi}_{\mathbf{k}}(1) \frac{\partial \tilde{p}_{\mathbf{k}'}}{\partial x_1}(1) \tilde{p}_{\mathbf{k}''}(2) + ik'_y \frac{\partial \tilde{\phi}_{\mathbf{k}}}{\partial x_1}(1) \tilde{p}_{\mathbf{k}'}(1) \tilde{p}_{\mathbf{k}''}(2) \Big) \Big] \Big\rangle + \langle 1 \leftrightarrow 2 \rangle. \end{aligned} \tag{51}$$

The average $\langle \cdots \rangle$ can be computed by integrating over the average position variables y_+ and z_+. After eliminating the trivial summation, the triplet can then be expressed in terms of test ($\mathbf{k}$), background ($\mathbf{k}'$), and driven beat ($\mathbf{k}'' = \mathbf{k} + \mathbf{k}'$) modes. The driven fluctuations are iteratively determined, using the solution for the driven fields given in Eqs. (28)–(30). As discussed in Sec. II, we neglect the driven potential fluctuation $\tilde{\phi}_{\mathbf{k}+\mathbf{k}'}$ and make a Markovian approximation ($\Delta\omega_{\mathbf{k}''} \sim \Delta\omega_{\mathbf{k}'}$) in the driven propagator, thus obtaining the renormalized triplet

$$T_{12} = -\left(D^x_- \frac{\partial^2}{\partial x^2_-} + D^y \frac{\partial^2}{\partial y^2_-} \right) \langle \mathscr{E}_{12} \rangle, \tag{52}$$

where the relative diffusion coefficients are given by

$$D^x_- = 2D^x - D^{x(1,2)} - D^{x(2,1)} \tag{53}$$

and

$$D^y_- = 2D^y - D^{y(1,2)} - D^{y(2,1)}, \tag{54}$$

with $D^x = D_k$ and $D^y = C_k$ in the expression of Eqs. (31)–(33) and

$$(D^{x(1,2)} + D^{x(2,1)}) = 2\sum_{k'} \cos(k' \cdot x_-) \frac{(k'_y)^2 \langle \tilde{\phi}_{-k'}(1)\tilde{\phi}_{k'}(2)\rangle}{\Delta\omega_{k'}},$$

$$(D^{y(1,2)} + D^{y(2,1)}) = 2\sum_{k'} \cos(k' \cdot x_-) \frac{\langle \partial\tilde{\phi}_{-k'}/\partial x_1(1) \cdot \partial\tilde{\phi}_{k'}/\partial x_2(2)\rangle}{\Delta\omega_{k'}}.$$

Here, the renormalized triplet approximates the **E×B** turbulent mixing and mode coupling as a relative diffusion across the magnetic field. The resulting relative diffusions, D^x_- and D^y_-, are inhomogeneous and are seen to consist of two parts, scale-independent diffusion, D^x and D^y, same as one-point case, and scale-dependent correlated diffusion, $D^{(2,1)}$ and $D^{(1,2)}$, which accounts for incoherent mode coupling. These inhomogeneities of relative diffusion show that triplet behavior as 1→2 is correctly accounted for in the renormalization procedure. The inhomogeneity of relative diffusion with respect to relative separation is illustrated in Fig. 3.

The characteristic spatial scale is referred to as correlation scale for which $D^{(1,2)}$ and $D^{(2,1)}$ differ from zero. The correlation peaks when the relative separation is less than correlation scale. For relative separation less than the corresponding correlation scale, i.e., $|k_0 \cdot x_-| < 1$, where k_0 is the spectrum-averaged wavenumber (i.e., typical wavenumber of fluctuations), the relative diffusion coefficients, D^x_- and D^y_-, can be approximated by expanding the relative variables

$$D^{(x,y)}_- \simeq 2D^{(x,y)}(k^2_{0x}x^2_- + k^2_{0y}y^2_- + k^2_{0z}z^2_-),$$

where k_{0x}, k_{0y}, and k_{0z} are the spectrum-averaged wavenumbers in the x, y, and z directions, respectively.

Having renormalized the triplet nonlinearity, we also need to express the parallel viscous diffusion term as a dissipation operator for energy correlation in the relative coordinate. Using the equipartitioning assumption, we first write the dissipation term as a Fourier expansion in the y and z directions at each radial position, i.e.,

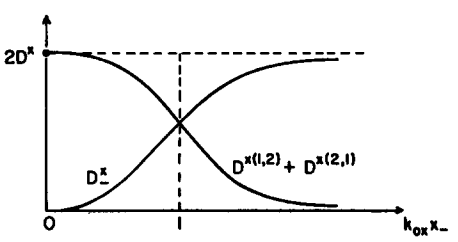

FIG. 3. Illustration for the inhomogeneity of relative diffusion coefficient to the normalized relative coordinate.

$$\langle S^I_{12}\rangle = \mu(\nabla^2_{\|1} + \nabla^2_{\|2})\langle \tilde{v}(1)\tilde{v}(2)\rangle \simeq \frac{\mu}{2}(\nabla^2_{\|1} + \nabla^2_{\|2})\langle \mathscr{E}_{12}\rangle$$

$$= \frac{\mu}{2}\Bigg\langle \sum_{k_1}\sum_{k_2} \exp(ik_{y1}y_1 + ik_{y2}y_2)\exp(ik_{z_1}z_1 + ik_{z_2}z_2) \times \left(\frac{[x_1 - x_s(k_1)]^2}{L_s^2}k^2_{y1} + \frac{[x_2 - x_s(k_2)]^2}{L_s^2}k^2_{y2}\right) \times (\mathscr{E}_{12})_{k_1,k_2}\Bigg\rangle. \tag{55}$$

To obtain this expression, recall that the wavenumbers corresponding to each position, $k_{y\alpha}$ and $k_{z\alpha}$ ($\alpha = 1,2$), and $\nabla_{\|\alpha}$ vanish at the rational surface associated with that position $x_s(k_\alpha)$, i.e.,

$$\frac{B_z}{B}k_{z\alpha} + \frac{B_y(x_s(k_\alpha))}{B}k_{y\alpha} = 0. \tag{56}$$

As before, the average $\langle\cdots\rangle$ produces Kronecker deltas $\delta_{k_{y1}+k_{y2}},0$, $\delta_{k_{z_1}+k_{z_2}},0$ which relate the two wave vectors ($k_1 = -k_2$). As a result, the double Fourier expansion is reduced to one in the relative variable. Furthermore, using the reflection invariance ($k \to -k$) of Eq. (56), it can be seen that both positions are tied to a single rational surface defined by $(B_z/B)k_z + [B_y(x_s)/B]k_y = 0$. Again, writing x_1 and x_2 in terms of the relative coordinates, the dissipation operator (in the spatial representation) is given by

$$(\mu/2)(\nabla^2_{\|1} + \nabla^2_{\|2})\langle \mathscr{E}_{12}\rangle = \frac{\mu}{4}\sum_k e^{ik_y y_- + ik_z z_-}\left(\frac{(x_+ - 2x_s)^2 + x^2_-}{L_s^2}\right)k^2_y\langle \mathscr{E}_{12}\rangle_k \simeq \frac{\mu}{4}\left(\frac{(x_+ - 2x_s)^2 + x^2_-}{L_s^2}\right)\frac{\partial^2}{\partial y^2_-}\langle \mathscr{E}_{12}\rangle. \tag{57}$$

Thus, the renormalized two-point equation is given by

$$\left[\frac{\partial}{\partial t} - \frac{\mu}{4}\left(\frac{(x_+ - 2x_s)^2}{L_s^2} + \frac{x^2_-}{L_s^2}\right)\frac{\partial^2}{\partial y^2_-} - \left(D^x_- \frac{\partial^2}{\partial x^2_-} + D^y_- \frac{\partial^2}{\partial y^2_-}\right)\right]\langle \mathscr{E}_{12}\rangle = \langle S^0_{12}\rangle, \tag{58}$$

where $\langle S^0_{12}\rangle$, the source term which accounts for fluctuation energy growth through average ion-pressure-gradient relaxation, is given by Eq. (50). Note that here, $(x_+ - 2x_s) \approx \Delta_k$, the turbulent correlation length.

In order to determine the steady-state spectrum, it is necessary to find the steady-state solution of Eq. (58). This requires inversion of the evolution operator

$$\mathscr{L} = \frac{\partial}{\partial t} - \frac{\mu}{4}\left(\frac{(x^2_+ - 2x_s)^2}{L_s^2} + \frac{x^2_-}{L_s^2}\right)\frac{\partial^2}{\partial y^2_-} - \left(D^x_- \frac{\partial^2}{\partial x^2_-} + D^y_- \frac{\partial^2}{\partial y^2}\right) \tag{59}$$

which describes the decay of correlation by relative diffusion due to **E×B** shear stress, and by parallel ion viscous dissipation. Formally, we can invert the evolution operator $\mathscr{L}$, and obtain the steady-state solution of Eq. (58) as

$$\langle \mathscr{E}_{12}\rangle = \tau_{cl}(x_-, y_-)\langle S^0_{12}\rangle, \tag{60}$$

where the inverse operator $\tau_{cl}(x_-, y_-) = \mathscr{L}^{-1}$. The opera-

tor $\tau_{cl}(x_-, y_-)$ describes characteristic time associated with the evolution of two-point correlation, and depends on the relative separation of the two points.

A solution for τ_{cl} may be obtained using the Green's function g, satisfying the homogeneous equation

$$\mathscr{L} g(\mathbf{x}_-|\mathbf{x}'_-) = 0, \tag{61}$$

so that

$$\langle \mathscr{E}_{12} \rangle = \int d\mathbf{x}'_- \, g(\mathbf{x}_-|\mathbf{x}'_-) \langle S^0_{12}(\mathbf{x}'_-) \rangle.$$

Although obtaining an exact expression for the Green's function g is possible, it is usually very complicated. Hence, it is sufficient for our purposes to determine the characteristic time τ_{cl} associated with the evolution operator $\mathscr{L}$. This approximate correlation time τ_{cl} can be determined by calculating the moments of the Green's function, which are defined by

$$\langle A \rangle \equiv \int d^3x'_- \, A(\mathbf{x}'_-) g(\mathbf{x}_-|\mathbf{x}'_-).$$

A set of relative coordinate moment evolution equations can be obtained by taking the second moments of the Green's function and using the relation

$$\frac{\partial}{\partial t} g = \left[\frac{\mu}{4} \left(\frac{(x_+ - 2x_s)^2}{L_s^2} + \frac{x_-^2}{L_s^2} \right) \frac{\partial^2}{\partial y_-^2} + \left(D^x_- \frac{\partial^2}{\partial x_-^2} + D^y_- \frac{\partial^2}{\partial y_-^2} \right) \right] g$$

and integrating by parts. The resulting moment equations are

$$\frac{\partial}{\partial t}(k_{0x}^2 \langle x_-^2 \rangle) = 4 D_{\mathbf{k}} k_{0x}^2 (k_{0x}^2 \langle x_-^2 \rangle + k_{0y}^2 \langle y_-^2 \rangle + k_{0z}^2 \langle z_-^2 \rangle), \tag{62}$$

$$\frac{\partial}{\partial t}(k_{0y}^2 \langle y_-^2 \rangle) = \frac{\mu k_{0y}^2}{2L_s^2} [(x_+ - 2x_s)^2 + \langle x_-^2 \rangle] + 4 C_{\mathbf{k}} k_{0y}^2 (k_{0x}^2 \langle x_-^2 \rangle + k_{0y}^2 \langle y_-^2 \rangle + k_{0z}^2 \langle z_-^2 \rangle), \tag{63}$$

$$\frac{\partial}{\partial t}(k_{0z}^2 \langle z_-^2 \rangle) = 0. \tag{64}$$

By defining a relative separation normalized with correlation scale

$$R^2_-(t) \equiv k_{0x}^2 x_-^2(t) + k_{0y}^2 y_-^2(t) + k_{0z}^2 z_-^2(t), \tag{65}$$

and its moments

$$\langle R^2_-(t) \rangle \equiv k_{0x}^2 \langle x_-^2 \rangle + k_{0y}^2 \langle y_-^2 \rangle + k_{0z}^2 \langle z_-^2 \rangle,$$

the resulting evolution equation of relative separation is

$$\frac{\partial^2}{\partial t^2} \langle R^2_- \rangle - 4(D_{\mathbf{k}} k_{0x}^2 + C_{\mathbf{k}} k_{0y}^2) \frac{\partial}{\partial t} \langle R^2_- \rangle - \frac{2\mu k_{0y}^2}{L_s^2 k_{0x}^2} \times (D_{\mathbf{k}} k_{0x}^2) \langle R^2_- \rangle = 0. \tag{66}$$

It is desirable to define a Reynolds number and other relevant parameters using the correlation scale $\mathbf{k}_0$. Therefore, let the Reynolds number be defined as

$$\mathrm{Re} \equiv \frac{[D_{\mathbf{k}} k_{0x}^2]}{[\mu k_{0y}^2 / (L_s^2 k_{0x}^2)]} = \frac{\tau_{d,\mathbf{k}}}{\tau_{c,\mathbf{k}}},$$

where $D_{\mathbf{k}}$ is the scale-independent radial diffusion coefficient, and τ_c is the coherent (one-point) relaxation time, and is given by $\tau_{c,\mathbf{k}}^{-1} = D_{\mathbf{k}} k_{0x}^2$ in the high Reynolds number limit. Here τ_d is the parallel dissipation time and is given by $\tau_{d,\mathbf{k}}^{-1} = [\mu k_{0y}^2 / (L_s^2 k_{0x}^2)]$. By parametrizing the ratio between scale-independent diffusion in the x and y directions as $\delta \equiv (C_{\mathbf{k}} k_{0y}^2 / D_{\mathbf{k}} k_{0x}^2)$, the evolution equation, Eq. (66), can be rewritten as

$$\frac{\partial^2}{\partial t^2} \langle R^2_- \rangle - \frac{4(1+\delta)}{\tau_c} \frac{\partial}{\partial t} \langle R^2_- \rangle - \frac{2}{\tau_d \tau_c} \langle R^2_- \rangle = 0. \tag{67}$$

Equation (67) describes the divergence of neighboring fluid elements by the turbulent scattering at high Reynolds numbers. At the small scales, however, scattering is damped by parallel dissipation.

The solution of the evolution equation is obtained as an initial value problem in which the initial separation is given by the second moments, i.e.,

$$\{\langle x_-^2 \rangle, \langle y_-^2 \rangle, \langle z_-^2 \rangle\}\big|_{t=0} = \{x_-^2, y_-^2 z_-^2\}, \tag{68}$$

and hence, $\langle R^2_- \rangle|_{t=0} = R^2_-$ determines the first and second derivatives of $\langle R^2_- \rangle$ at the initial time:

$$\frac{\partial}{\partial t} \langle R^2_-(t) \rangle \Big|_{t=0} = \frac{4(1+\delta)}{\tau_c} R^2_- + \frac{k_{0x}^2}{2\tau_d} \times [(x_+ - 2x_s)^2 - x_-^2], \tag{69}$$

and

$$\frac{\partial^2}{\partial t^2} \langle R^2_-(t) \rangle \Big|_{t=0} = \left(\frac{16(1+\delta)^2}{\tau_c^2} + \frac{2}{\tau_c \tau_d} \right) R^2_- + \frac{2(1+\delta)}{\tau_c \tau_d} k_{0x}^2 [(x_+ - 2x_s)^2 + x_-^2]. \tag{70}$$

Then, the solution of Eq. (67) is given by

$$\langle R^2_-(t) \rangle = A e^{u_+ t} + B e^{u_- t}, \tag{71}$$

where $u_\pm$ are the two roots of the characteristic equation generated by trial solution e^{ut}:

$$u^2 - [4(1+\delta)/\tau_c] u - 2/\tau_c \tau_d = 0. \tag{72}$$

The two roots are given by

$$u_\pm = \frac{2(1+\delta)}{\tau_c} \left(1 \pm \sqrt{1 + \frac{\mathrm{Re}^{-1}}{2(1+\delta)^2}} \right).$$

The coefficients, A and B, are determined by requiring that Eq. (67) satisfies the initial conditions Eqs. (68)–(70). Thus

$$A = (u_+ - u_-)^{-1} \left[\left(\frac{1}{u_+} \right) \frac{\partial^2}{\partial t^2} \langle R^2_- \rangle \Big|_{t=0} - \left(\frac{u_-}{u_+} \right) \frac{\partial}{\partial t} \langle R^2_- \rangle \Big|_{t=0} \right], \tag{73}$$

$$B = (u_+ - u_-)^{-1}\left[\left(\frac{u_+}{u_-}\right)\frac{\partial}{\partial t}\langle R^2_-\rangle\Big|_{t=0} - \left(\frac{1}{u_-}\right)\frac{\partial^2}{\partial t^2}\langle R^2_-\rangle\Big|_{t=0}\right]. \quad (74)$$

For initial separations which are much smaller than the spatial correlation scale, $|\mathbf{k}_0\cdot\mathbf{x}_-|\ll 1$, the time t will become large before relative separation reaches the correlation scale, i.e., $|\mathbf{k}_0\cdot\mathbf{x}_-|\simeq 1$. Then we may approximate the solution with the time-asymptotically dominant piece, which is (noting that $u_- < 0$)

$$\langle R^2_-(t)\rangle \simeq Ae^{u_+ t}. \quad (75)$$

Here, the coefficient A can be calculated straightforwardly using Eq. (73), which yields

$$A = \frac{[(1+\epsilon/2)+\sqrt{1+\epsilon}]}{\sqrt{1+\epsilon}(1+\sqrt{1+\epsilon})}\{\alpha k_{0x}^2(x_+ - 2x_s)^2 + (1+\alpha)k_{0x}^2 x_-^2 + k_{0y}^2 y_-^2 + k_{0z}^2 z_-^2\}, \quad (76)$$

where Reynolds-number-dependent numerical parameters are defined by $\epsilon = \mathrm{Re}^{-1}/[2(1+\delta)^2]\to 0$ as $\mathrm{Re}\to\infty$, and $\alpha = \epsilon(1+\delta)(1+\sqrt{1+\epsilon})/4[1+\epsilon/2)+\sqrt{1+\epsilon}]\to 0$ as $\mathrm{Re}\to\infty$. When time t is of the order of the correlation time τ_{cl}, the relative separation reaches the correlation scale, i.e., $\langle R^2_-(t)\rangle|_{t=\tau_{cl}}\simeq 1$. Using this condition, the two-point correlation lifetime can be determined by solving for t in Eq. (75), thus yielding

$$\tau_{cl} = \frac{-\tau_c}{2(1+\delta)[1+\sqrt{1+\epsilon}]}\ln\{C[\alpha k_{0x}^2(x_+ - 2x_s)^2 + (1+\alpha)k_{0x}^2 x_-^2 + k_{0y}^2 y_-^2 + k_{0z}^2 z_-^2]\}, \quad (77)$$

where $C = [(1+\epsilon/2)+\sqrt{1+\epsilon}]/\sqrt{1+\epsilon}(1+\sqrt{1+\epsilon})\to 1$ as $\mathrm{Re}\to\infty$. The factor multiplying the logarithm in the expression of τ_{cl} represents the large separation coherence time, retaining finite Reynolds number effects.

For Reynolds number exceeding order unity, the logarithmic function yields peaked correlation functions for small initial separations. The peaking becomes increasingly pronounced as the Reynolds number increases. The correlation scales are determined by the coefficients of the relative coordinate in the logarithm. The radial scale of correlation can be deduced, and is given by

$$\Delta_x \simeq (1+\alpha)^{-1/2}C^{-1/2}k_{0x}^{-1},$$

where k_{0x}^{-1} is the (nonlinear) radial mode width (mixing length). This radial scale incorporates finite Reynolds number corrections to the mixing-length estimate through the parameters α and C, which are functions of Reynolds number. The result of the mixing-length theory can be recovered for $\mathrm{Re}\to\infty$ limit, i.e., $\Delta_x \simeq k_{0x}^{-1} = \Delta_k$ as $\mathrm{Re}\to\infty$. The correlation scale in the y direction is k_{0y}^{-1}, which corresponds to an inverse of the typical wavelength in the fluctuation spectrum. It is also important to notice that the one-point response correctly reduced to the coherent turbulent response in the limit of large Reynolds number. This limit is assumed in the mixing-length theory. The "inertial" range corresponds to scales for which $\mathrm{Re}\gg 1$, and represents a regime where the nonlinear effect dominates the dissipation in the two-point equation, and for which the dynamics is conservative. Also in this limit, the parameter α approaches zero and the correlation is singular at zero initial separation. For finite Reynolds number regimes, the correlation function is finite even with zero initial separation, because parallel dissipation contributes through the $\alpha k_{0x}^2(x_+ - 2x_s)^2$ term. The "dissipation" range k_y spectrum can be estimated using the definition of Reynolds number and setting $\mathrm{Re}\sim 1$ for the dissipation range wavenumber, that is, in the dissipation range the linear parallel dissipation is comparable to nonlinear effects. This yields $(k_y)_d \simeq \sqrt{\mathrm{Re}}k_{0y}$, where $(k_y)_d$ is the dissipation range wavenumber.

It is worthwhile to note here that the correlation boundary can be defined by

$$C\{\alpha k_{0x}^2(x_+ - 2x_s)^2 + (1+\alpha)k_{0x}^2 x_-^2 + k_{0y}^2 y_-^2 + k_{0z}^2 z_-^2\} = 1. \quad (78)$$

In the normalized relative coordinates, this forms an ellipsoidal surface for finite Reynolds number. For the case of infinite Reynolds number, this correlation boundary is a spherical surface with radius unity in normalized relative coordinates.

Using τ_{cl} given in Eq. (77), we can obtain the stationary spectrum equation from the steady-state solution of the two-point energy correlation equation,

$$\langle \mathscr{E}_{12}\rangle \simeq \tau_{cl}\langle S^0_{12}\rangle.$$

In order to calculate the steady-state wavenumber spectrum from the stationary spectrum equation, it is necessary to express the source $\langle S^0_{12}\rangle$ in terms of $\langle \mathscr{E}_{12}\rangle$ by using the steady-state condition in Eq. (35) and the equipartitioning assumption. This yields

$$\langle S^0_{12}\rangle \simeq \sum_{\mathbf{k}}\left(\frac{1+\eta_i}{\tau}\right)\frac{|k_y|}{L_s}\langle \mathscr{E}_{12}(x_-)\rangle_{\mathbf{k}} e^{ik_y y_-}e^{ik_z z_-}. \quad (79)$$

Since two points are well correlated only if the relative separation is small compared to correlation scales, i.e., $|\mathbf{k}_0\cdot\mathbf{x}_-|\ll 1$, the approximation $\exp(ik_y y_- + ik_z z_-)\simeq 1$ is employed and the x_- dependence in $\langle \mathscr{E}_{12}(x_-)\rangle_{\mathbf{k}}$ is also neglected in the source term for the high Reynolds number regime. Thus, we can rewrite the stationary spectrum equation as

$$\langle \mathscr{E}_{12}(x_-,y_-,z_-)\rangle \simeq \tau_{cl}(x_-,y_-,z_-)\langle S^0\rangle, \quad (80)$$

where $\langle S^0\rangle$ is the source term evaluated with these approximations.

Since $\langle S^0\rangle$ is now independent of the relative coordinate $\mathbf{x}_-$, the wavenumber spectrum of the energy correlation can be determined by the Fourier transform of $\tau_{cl}(x_-,y_-,z_-)$. After Fourier transforming both sides of Eq. (80) in the y and z directions, and taking an x_- average over radial correlation length Δ_x, we obtain

$$\langle \mathscr{E}_{12}\rangle_{\mathbf{k}} = \frac{1}{2\Delta_x}\left(\frac{1}{2\pi}\right)\int_{-\Delta_x}^{\Delta_x} dx_- \int dy_- \int dz_-\, \bar{\tau}_{cl}(x_-,y_-,z_-) \times \langle S^0\rangle e^{-ik_y y_-}e^{-ik_z z_-}, \quad (81)$$

where

$$\bar{\tau}_{\rm cl}(x_-,y_-,z_-) = \tau_{\rm cl}(x_+,x_-,y_-,z_-)\,\big|_{(x_+-2x_s)=\Delta_x}.$$

Since the expression for $\tau_{\rm cl}$ loses its meaning and validity when the argument of the logarithm is larger than unity, it is necessary to restrict the range of integration to within the correlation boundary, as given by Eq. (78). The integration can be performed using a Fourier–Bessel expansion and the summation theorem of Bessel functions. This yields

$$(\bar{\tau}_{\rm cl})_{\mathbf{k}} \equiv \frac{1}{2\Delta_x}\int_{-\Delta_x}^{\Delta_x} dx_- \int dy_- \int dz_- \times \bar{\tau}_{\rm cl}(x_-,y_-,z_-)e^{-ik_y y_-}e^{-ik_z z_-} = \frac{\tau_c}{2(1+\delta)\,(1+\sqrt{1+\epsilon})}F(k_y,k_z), \tag{82}$$

where

$$F(k_y k_z) = -\frac{1}{\Delta_x}\int_0^{\Delta_x} dx_- \int dy_- \int dz_-\, e^{-ik_y y_-}e^{-ik_z z_-}\ln\left[\left(\frac{\alpha}{\alpha+1}\right)+C\left[(1+\alpha)k_{0x}^2x_-^2+k_{0y}^2y_-^2+k_{0z}^2z_-^2\right]\right]$$
$$= \left(\frac{4\pi}{Ck_{0y}k_{0z}}\right)\int_0^{\xi}(\sqrt{\xi^2-\rho^2}-\sqrt{1+\rho^2-\xi^2}\cos^{-1}\sqrt{1+\rho^2-\xi^2})\rho J_0\left(\frac{\beta\rho}{\sqrt{C}}\right)d\rho, \tag{83}$$

with $\xi=\sqrt{1/(1+\alpha)}$ and $\beta=\sqrt{(k_y/k_{0y})^2+(k_z/k_{0z})^2}$. Details of these integrations are given in Appendix A. Hence, the inertial range energy k_y spectrum can be calculated by taking the Re$\to\infty$ limit and summing over k_z, yielding

$$\langle \mathscr{E}_{12}\rangle_{k_y} \simeq 2\int_0^{\infty} dk_z \langle \mathscr{E}_{12}\rangle_{\mathbf{k}} = \frac{2\pi k_{0y}}{k_y^2}\left[1-J_0\left(\frac{k_y}{k_{0y}}\right)\right]\langle S^0\rangle. \tag{84}$$

The wavenumber dependence of the energy spectrum fits a power law of the form

$$\langle \mathscr{E}_{12}\rangle_{k_y} \sim k_y^{-5/2}$$

in the first decade of decay from its peak value.

Numerical evaluations of the k_y-wavenumber spectrum of energy correlation for the two cases (Re = 5 and Re$\to\infty$) are plotted in Fig. 4. In the low-k_y region of the spectrum, $\langle \mathscr{E}_{12}\rangle_{k_y} \simeq k_y^0$ and exhibits an energy-containing range structure. In the $k_y \simeq k_{0y}$ range, the spectrum falls off according to the power law and exhibits an inertial range structure. Finally, for $k_y \simeq 6k_{0y}$, $\langle E_{12}\rangle_{k_y}$ is oscillatory due to the approximation used to cut off $\tau_{\rm cl}$ at the correlation boundary. This oscillation indicates a breakdown of the approximations at high k_y. However, the energy content of the spectrum in this range is negligible, and this region falls in the dissipation range $k_y > (k_y)_d$. Therefore, these oscillations are of no consequence.

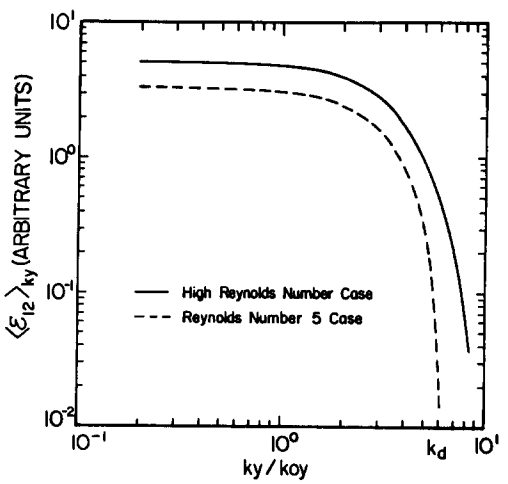

FIG. 4. Wavenumber spectrum of energy correlation for the high Reynolds number and Re = 5 cases.

Now, we can compare the results of the two-point theory with predictions of one-point mixing-length theory. Noting the source can be written as

$$\langle S^0\rangle \simeq \sum_{\mathbf{k}'}\left(\frac{1+\eta_i}{\tau}\right)\frac{|k_y'|}{L_s}\langle \mathscr{E}_{12}\rangle_{\mathbf{k}'}$$

and multiplying by (k_y/k_{0y}), and integrating both sides of Eq. (81) over k_y and k_z, and solving for D^x yields

$$D^x \simeq \left(\frac{\pi^2}{4(1+\delta)^2}[\ln(1+\eta_i)]^2\right)\left(\frac{k_{0y}}{L_s}\right)\left(\frac{1+\eta_i}{\tau}\right)^2. \tag{85}$$

This result has identical scalings to the results of one-point theory, but contains an additional numerical multiplier given in brackets, which depends on Reynolds number, i.e.,

$$\mathrm{Re} = [D_{\mathbf{k}}k_{0x}^2]/[\mu k_{0y}^2/(L_s^2 k_{0x}^2)] \simeq (1+\eta_i).$$

Even though the additional multiplier is order unity and a weak function of Reynolds number (this multiplier has numerical value of order 5 for η_i values of experimental interest), it is very important to notice that this multiplier is crucial for a description of steady-state turbulence because it depends on dissipation through the definition of Reynolds number. Because the transport coefficients, such as diffusivity and conductivity, depend on spectral sum of fluctuation amplitudes, it is necessary to determine the integration range of the spectrum (i.e., dissipation range wavenumber) even for high Reynolds number turbulence. The theories based only on the inertial range structure of high Reynolds number turbulence, such as the mixing-length theory and the scale transformation technique,[11] may estimate transport scalings. However, those theories fail to represent the crucial property of the steady-state condition associated with dissipation.

Having derived the wavenumber spectrum of fluctuations, one can evaluate the spectrum-averaged wavenumber of η_i mode turbulence [i.e., $(k_y)_{\rm rms} = k_{0y}$] by taking the rms value of the k_y wavenumber, i.e.,

$$(k_y)_{\rm rms} \equiv \left[\frac{\Sigma_{k_y} k_y^2 \langle \mathscr{E}_{12} \rangle_{k_y}}{\Sigma_{k_y} \langle \mathscr{E}_{12} \rangle_{k_y}}\right]^{1/2}. \quad (86)$$

The integration of Eq. (86) shows that $(k_y)_{\rm rms}$ is a weak function of Reynolds number and has a numerical value of 0.4 (in ρ_s^{-1} unit) for the η_i value to which the fluid model is applicable. This typical wavenumber can only be calculated by using two-point theory. The other theories based on one-point renormalization or on scale transformation effectively treat this wavenumber as a free parameter.

Using the predicted diffusion level,Eq. (85), and the rms wavenumber, the mean-squared radial velocity can be estimated as

$$(\tilde{v}_r)_{\rm rms} \equiv \sqrt{\overline{E}_{\mathbf{k}}} \simeq \left(\frac{\pi^2}{4(1+\delta)^2}[\ln(1+\eta_i)]^2\right) \times \left(\frac{k_{0y}}{L_s}\right)\left(\frac{1+\eta_i}{\tau}\right)^{3/2}. \quad (87)$$

The principal results of this section are the calculations of the two-point energy correlation function, the wavenumber spectrum of the ion pressure fluctuations, and the ion thermal diffusivity and average wavenumber. To summarize these results, the energy spectrum dependence on poloidal wavenumber is given by

$$\langle \tilde{P}_i^2 \rangle_{k_\theta} \simeq k_\theta^{-5/2},$$

with the spectrum-averaged poloidal wavenumber being $(k_\theta \rho_s)_{\rm rms} \simeq 0.4$. The ion thermal diffusivity is given by

$$\chi_i \simeq \left(\frac{\pi^2}{4}[\ln(1+\eta_i)]^2\right)\left(\frac{1+\eta_i}{\tau}\right)^2 \frac{(k_\theta \rho_s)_{\rm rms}}{L_s} \rho_s^2 c_s.$$

The predicted rms values of fluctuating radial velocity, pressure, and potential are

$$(\tilde{v}_r)_{\rm rms} \simeq \left(\frac{\pi^2}{4}[\ln(1+\eta_i)]^2\right)\left(\frac{1+\eta_i}{\tau}\right)^{3/2} (k_\theta \rho_s)_{\rm rms} \frac{\rho_s c_s}{L_s},$$

and

$$\left(\frac{\tilde{P}_i}{P_{0i}}\right)_{\rm rms} \simeq \left(\frac{\pi^2}{4}[\ln(1+\eta_i)]^2\right)\left(\frac{1+\eta_i}{\tau}\right)^{3/2} \frac{\rho_s}{L_n},$$

and

$$\left(\frac{\tilde{n}}{n_0}\right)_{\rm rms} = \left(\frac{e\Phi}{T_e}\right)_{\rm rms} \simeq \left(\frac{\pi^2}{4}[\ln(1+\eta_i)]^2\right)\left(\frac{1+\eta_i}{\tau}\right)^{3/2} \frac{\rho_s}{L_s},$$

respectively.

IV. APPLICATIONS: HEAT AND PARTICLE TRANSPORT IN TOKAMAKS

Having obtained the wavenumber spectrum and fluctuation levels at saturation, we now consider the effect of η_i-mode turbulence on heat and particle transport in tokamak experiments.

A. Ion and electron thermal conduction

Recent experimental results from the Alcator-C tokamak[1,2] have indicated that in the high-density saturated electron confinement regime of Ohmically heated discharges, in which the electron energy confinement time τ_E ($\propto n$) approaches or exceeds the equilibrium time between electrons and ions τ_{ei} ($\propto 1/n^2$), there is an anomalous ion heat loss which is apparently related to large η_i values (i.e., $\eta_i > \eta_{ic}$ observed). This is also consistent with the observation that the injection of a large pellet and the subsequent density gradient steepening result in an improvement in energy confinement. There is also an indication of anomalous ion heat conductivity in neutral beam heated, density-clamped (L-mode) tokamak experiments (e.g., D-III tokamak[3]). In this case, beam injection directly heats the ions while simultaneously, particle confinement degrades. This results in an increase in η_i. For the L phase of D-III, the result of transport analyses with measured ion temperature profiles (determined by charge exchange recombination spectroscopy) indicate significant departure from neoclassical ion heat conductivity values $\chi_i^{\rm Neo}$.[21] Also, the radial dependence of χ_i is not related to $\chi_i^{\rm Neo}$ (see Ref. 3). It is plausible to explore an interpretation of this anomaly as η_i-mode turbulence driven ion conduction heat loss.

The anomalous ion thermal conductivity can be calculated in a straightforward manner, by using the saturation level of fluctuations. The ion thermal flux $q(r)$ due to $\mathbf{E}\times\mathbf{B}$ turbulent convection of perturbed ion pressure is given in terms of the pressure-potential cross correlation by

$$q_i = -\langle \tilde{p}_i \nabla_y \tilde{\phi} \rangle = \sum_{k_y} (-ik_y) \langle \tilde{p}_i \tilde{\phi} \rangle_{k_y}. \quad (88)$$

Using the decorrelation rate $[D^x/(\Delta_x)^2]$ given in Eq. (85), the integrated radial velocity $\overline{E}$ in Eq. (87), and the definition of ion thermal conductivity

$$q_i(r) = \tau \sum_{k_y} \left(\frac{1+\eta_i}{\tau}\right)\frac{k_y^2}{L_n} |\tilde{\phi}_{\mathbf{k}}|^2 \Big/ \left(\frac{D^x}{(\Delta_x)^2}\right). \quad (89)$$

Using the decorrelation rate $[D^x/(\Delta_x)^2]$ given in Eq. (85), the integrated radial velocity $\overline{E}$ in Eq. (87), and the definition of ion thermal conductivity

$$\chi_i(r) \equiv -q_i(r) \Big/ \left(\frac{d\langle P_{0i} \rangle}{dr}\right), \quad (90)$$

we find the final form of the anomalous ion thermal conductivity to be (for $\eta_i > \eta_{ic} \sim 1.5$).

$$\chi_i \simeq \left(\frac{\pi^2}{4}[\ln(1+\eta_i)]^2\right)\frac{(k_y)_{\rm rms}}{L_s}\left(\frac{1+\eta_i}{\tau}\right)^2. \quad (91)$$

In dimensional units, χ_i can be expressed as

$$\chi_i \simeq \left(\frac{\pi^2}{4}[\ln(1+\eta_i)]^2\right)\frac{(k_y \rho_s)_{\rm rms}}{L_s}\left(\frac{1+\eta_i}{\tau}\right)^2 \rho_s^2 c_s, \quad (92)$$

where the mean wavenumber $(k_y \rho_s)_{\rm rms} \simeq 0.4$.

For the case of nearly flat density profiles observed in the ohmic saturation regime of the Alcator-C tokamak, [$\eta_i \simeq 4$, $T_i \simeq 700$ eV ($T_i \simeq T_e$), and $B_0 \simeq 9T$ for $r = a/2$] the ion thermal conductivity due to η_i-mode turbulence is approximately 4.0×10^3 cm^2/sec. Here, it is very important to note

that the Reynolds number dependent multiplier (from spectrum summation) $((\pi^2/4)[\ln(1+\eta_i)]^2)$ has a numerical value of 6.4 for given parameters, and this numerical factor is important for quantitative evaluation of χ_i, even though this multiplier is a weak (logarithmic) function of η_i. Also, note that the scaling $\chi_i \sim (1+\eta_i)^2$ implies that large values of η_i are unlikely and that L_{T_i} is a weak function of ion heating power P_I (i.e., thermal balance implies $L_{T_i} \simeq P_I^{-1/3}$), so that $T_i(r)$ profiles remain comparatively similar. This is consistent with observed $\eta_i(r)$ profiles from the L-phase regime of the ASDEX tokamak, where $\eta_{ic} < \eta_i \lesssim 3$.[22]

Another application of η_i-mode turbulence driven anomalous ion heat loss has been proposed in the context of a high current reversed field pinch (RFP) by An *et al.*[33] They studied a coupled system of resistive-interchange and ion-temperature-gradient-driven turbulence, and reported the possibility of significant ion thermal loss in a high current, high temperature RFP. This coupled system might also be relevant to the understanding of anomalous heat transport in stellarators.

In a tokamak plasma, in addition to (direct) ion heat loss, there is a possible electron thermal loss associated with the dissipative trapped electron response ($\nu_* < 1$) to η_i-mode turbulence. In the trapped-electron regime (i.e., $\nu_{*e} < 1$, $\nu_{*e} \equiv \nu_{\text{eff},e}/\omega_{be}$) of tokamak plasmas, the presence of trapped electrons can result in a heat flux associated with background fluctuations driven by the η_i-mode turbulence. It is well known[24] that for $\nu_{*e} < 1$, the perturbed distribution for trapped electrons is

$$f_e^T = \frac{eF_{Me}}{T_e}\left(\Phi - \frac{\omega - \omega_{*e}[1+\eta_e(E/T_e - 3/2)]}{\omega - \bar{\omega}_{De} + i\nu_{\text{eff},e}}\bar{\Phi}\right), \tag{93}$$

with $\bar{\Phi} \equiv$ trapped-particle-orbit-averaged electrostatic potential. The anomalous electron heat flux can be estimated by using

$$(Q_r^e)^T \simeq \langle (\tfrac{1}{2}mv_e^2)[\tilde{n}\tilde{v}_{Er}]\rangle^T, \tag{94}$$

where $\langle \cdots \rangle^T$ represents the velocity-space average over trapped electrons. For a simple estimate of the trapped-electron contribution, the bounce average can be ignored and the resulting heat flux is given by

$$(Q_r^e)^T \simeq -n_{0e}(15\sqrt{2})\epsilon^{3/2}(k_y^2\rho_s^2)\frac{c_s^2}{\nu_e}\frac{dT_e}{dr}\left|\frac{e\Phi}{T_e}\right|^2 \tag{95}$$

in the high-collisionality limit of the banana regime where ω, $\bar{\omega}_{De} \ll \nu_{\text{eff},e}$ and $\eta_i \simeq \eta_e \gg 1$. Using the saturation amplitude of the radial velocity of the η_i-mode turbulence given by Eq. (87), the electron heat conductivity is given by

$$\chi_e \simeq 15\sqrt{2}\epsilon^{3/2}\left(\frac{\pi}{2}\ln(1+\eta_i)\right)^4\left(\frac{1+\eta_i}{\tau}\right)^3\left(\frac{c_s^2\rho_s^2}{\nu_e L_s^2}\right) \times (k_y^2\rho_s^2)_{\text{rms}}, \tag{96}$$

where ϵ is the inverse aspect ratio and the mean wavenumber has been used to evaluate χ_e [$(k_y\rho_s)_{\text{rms}} = 0.4$]. Thus, ion-temperature-gradient-driven turbulence can also result in increased anomalous electron thermal conduction. However, while there is certainly a relation between the resulting χ_i and χ_e, they clearly scale quite differently and cannot be arbitrarily assumed to be comparable. In particular, for $\epsilon^{3/2}c_s/L_s\nu_e < 1$, $\chi_e < \chi_i$.

B. Particle transport

1. Ion-mixing driven particle influx

As in the case of the high-density saturation regime of the Alcator-C tokamak experiment, there have been many gas-fueled tokamaks that exhibit an anomalous inward density pinch after puffing of neutral gas into the plasma chamber. Previously, the theory of the ion-mixing mode[5] has been proposed to explain this anomalous inward particle flux. The coupling of ion-temperature-gradient-driven modes to a collisional electron response is thought to be responsible for this anomaly. However, as discussed previously, the estimate of the saturation level used in Ref. 5 (invoking the heuristic ambient-gradient-type argument) is probably incorrect. Here, we reexamine the ion-mixing driven particle transport using the results of the η_i-mode turbulence calculation that has been presented in previous sections.

In the η_i-mode turbulence theory, the electron density response has been approximated as adiabatic. Because the density and radial velocity are 90° out of phase in the adiabatic approximation, no particle transport can result. However, when considering near-edge tokamak plasma where the anomalous inward particle pinch is significant, finite electron parallel thermal conductivity due to collisions is not negligible. Thus, the nonadiabatic part of the electron density response should be retained. It can provide a phase difference between $\tilde{n}$ and $\tilde{\phi}$, thus giving rise to net particle transport.

For the wide range of collisionality regimes that are appropriate for near-edge tokamak parameters, the electron fluid equations[13] can be applied to calculate the (electron) density response. Also, by comparing the radial scale length of the collisional electron response Δ_k^c[6] with nonlinear η_i-mode radial mixing scale Δ_k, it can be shown that the linear electron response is an adequate approximation (i.e., $\Delta_k^c < \Delta_k$). A laborious but straightforward calculation shows that the electron density response is given by

$$\tilde{n}_e/n_0 = A(\mathbf{k},\omega)\tilde{\phi}, \tag{97}$$

where

$$A(\mathbf{k},\omega) \equiv \frac{\left(\left[\tfrac{3}{2}\hat{\chi}_e(\omega_{*e}/\omega) - \omega_\chi^2/\omega^2\right] + i\left\{\tfrac{3}{2}\omega_\chi/\omega + \left[\hat{\chi}_e + (1+\alpha_T)^2 - \tfrac{3}{2}(1+\alpha_T)\eta_e\right](\omega_{*e}\omega_\chi/\omega^2)\right\}\right)}{\left[\left(\tfrac{3}{2}\hat{\chi}_e - \omega_\chi^2/\omega^2\right) + i\left(\tfrac{3}{2} + \hat{\chi}_e + (1+\alpha_T)^2\right)(\omega_\chi/\omega)\right]}, \tag{98}$$

and

$$\omega_\chi \equiv (\hat{\chi}_e/0.51)\,(T_{e0}/m_e\nu_e)k_\parallel^2 \tag{99}$$

with numerical factors of $\hat{\chi}_e = 1.61$ and $\alpha_T = 0.71$ for $k_\parallel v_{\mathrm{th},e} < \nu_e$. For the regime where

$$\left(\frac{\overline{\omega_\chi}}{\omega_{*e}}\right) = \left(\frac{\hat{\chi}_e}{0.51}\right)\left(\frac{m_i}{m_e}\right)\left(\frac{\overline{\omega_{*e}}}{\nu_e}\right)\left(\frac{L_n}{L_s}\right)^2\left(\frac{\overline{\Delta_r}}{\rho_s}\right)^2 \gg 1,$$

where the overbars indicate evaluation at a mean wavenumber and mean radial scale, the electron density response is almost adiabatic with a small nonadiabatic (imaginary) part due to electron thermal conductivity. Although the nonadiabatic part of electron density response is important for evaluating particle transport, it can be shown that this nonadiabatic electron response in the $(\omega_\chi/\omega_{*e}) \gg 1$ regime has little influence on the basic stability and the radial scale of the η_i-mode. Hence, the resulting particle flux can be quasilinearly calculated by using the saturated radial velocity level which has been determined in the context of η_i-mode turbulence.

Proceeding, the anomalous particle flux, Γ_r from $\mathbf{E}\times\mathbf{B}$ turbulent convection of the perturbed density is given in terms of the density-potential cross correlation by

$$\Gamma_r \simeq \langle \tilde{v}_{Er} \cdot \tilde{n} \rangle = -i\sum_{k_y} k_y \langle \tilde{\phi}\tilde{n} \rangle_{k_y}. \tag{100}$$

For the $(\overline{\omega_\chi/\omega_{*e}}) \gg 1$ regime, the particle flux is given by

$$\Gamma_r \simeq 2[\hat{\chi}_e + (1+\alpha_T)^2]\left(1 - \frac{\eta_e}{\eta_e^c}\right)\sum_{k_y} k_y \left(\frac{\omega_{*e}}{\omega_\chi}\right)|\tilde{\phi}_{\mathbf{k}}|^2, \tag{101}$$

where

$$\eta_e^c \simeq \left(\frac{\hat{\chi}_e + (1+\alpha_T)^2}{\frac{3}{2}(1+\alpha_T)}\right) \simeq 1.77.$$

Using the rms value of the radial velocity given in Eq. (87), the particle pinch velocity can be calculated (in dimensional units) and is

$$\langle V_r \rangle \equiv \frac{\Gamma_r}{n_0} \simeq \left(\frac{\pi^4}{8}[\ln(1+\eta_i)]^4\right)[\hat{\chi}_e + (1+\alpha_T)^2] \times \left(1 - \frac{\eta_e}{\eta_e^c}\right)\left(\frac{m_e}{m_i}\right)\frac{0.51}{\hat{\chi}_e}\frac{\nu_e}{L_n}\left(\frac{1+\eta_i}{\tau}\right)^2\rho_s^2. \tag{102}$$

It should be noticed, however, that the assumptions $k_\parallel v_{\mathrm{th},e} < \nu_e$ and $\eta_e > \eta_e^c$ must be satisfied for consistency and applicability of the theory (also, $\eta_i > \eta_{ic}$ must be satisfied for instability). But this inflow of particles is due to the off-diagonal element of flux-force transport relation, the critical value η_e^c represents competition between two opposing forces (namely dn/dr corresponding to particle diffusion, and dT/dr, which corresponds to the inward pinch).

For the case of near-edge parameters in the Alcator-C tokamak with $\eta_i \approx \eta_e \simeq 4$, $T_i \approx T_e \simeq 50$ eV, and $B \simeq 9$ T, the pinch velocity is approximately $\langle V_r \rangle \simeq 1000$ cm/sec.

For the collisional regime where $(\overline{\omega_\chi/\omega_{*e}}) > 1$, it is interesting to note that in addition to an inward flux of particles, there also exists a heat-pinch effect. Recently, the concept of a heat pinch has been proposed in order to explain the disparity between thermal diffusivities obtained from heat pulse propagation studies and transport analysis. This flow of electron heat can be determined from the electron pressure-potential cross correlation

$$Q_r^e \simeq \langle \tilde{v}_{Er} \cdot \tilde{P}_e \rangle, \tag{103}$$

where $\tilde{P}_e = \tilde{n}_e T_{e0} + n_0 \tilde{T}_e$. Thus,

$$Q_r^e = P_{e0}\left(\frac{\pi^4}{8}[\ln(1+\eta_i)]^4\right)[\hat{\chi}_e + (1+\alpha_T)^2] \times \left(1 - \frac{\eta_e}{\eta_e^{\mathrm{HP}}}\right)\left(\frac{m_e}{m_i}\right)\frac{0.51}{\hat{\chi}_e}\frac{\nu_e}{L_n}\left(\frac{1+\eta_i}{\tau}\right)^2\rho_s^2. \tag{104}$$

Electron heat can flow inward (heat-pinch) provided $\eta_e > \eta_E^{\mathrm{HP}}$ with $\eta_e^{\mathrm{HP}} = \frac{3}{2}(1 + \alpha_T + \hat{\chi}_e/\alpha_T) \simeq 2.65$. It should be noticed that the critical η_e value for a heat pinch is greater than the critical η_e value for a particle pinch because of the additional contribution from $\tilde{T}_e$.

For the central region of tokamaks that are characterized by low collisionality, the dissipative trapped-electron response[22] provides the necessary phase shift between the density response and fluctuating electrostatic potential for net particle transport. Using the expression for the perturbed distribution of trapped electrons in Eq. (93), the anomalous particle flux at low electron collisionality is given by

$$\Gamma_r^T \simeq \langle \tilde{v}_{Er} \cdot \tilde{n}_e \rangle \simeq \epsilon^{1/2} n_{0e} (k_{0y}\rho_s) c_s |e\phi/T_e|^2 \times \left(\frac{\omega_{*e}(1+\frac{3}{2}\eta_e) - \mathrm{Re}(\omega)}{(\nu_e/\epsilon)}\right). \tag{105}$$

Here, the high-collisionality limit of the banana regime, i.e., $\omega, \bar{\omega}_{De} \ll \nu_{\mathrm{eff},e}$ has been assumed. Using the rms value of the saturation amplitude of the fluctuating radial velocity of the η_i-mode turbulence given by Eq. (87), the average radial particle convection speed can be calculated and is

$$\langle V_r \rangle^T \simeq \Gamma_r^T/n_0 \simeq \epsilon^{3/2}\left[\frac{\omega_{*e}(1+\frac{3}{2}\eta_e) - \mathrm{Re}(\omega)}{\nu_e}\right] \times \left[\frac{\pi^2}{4}[\ln(1+\eta_i)]^2\right]^2\left(\frac{1+\eta_i}{\tau}\right)^3\frac{(k_y\rho_s)_{\mathrm{rms}}\rho_s^2 c_s}{L_s^2}. \tag{106}$$

This leads to the conclusion that the resulting particle flux (for $\eta_e > 0$) is always directed outward. This prediction of outward particle flow in low collisionality regimes might offer one possible explanation of the observed improved particle confinement after pellet injection. Such improvement would occur when outward particle flow is reduced after pellet-induced density profile steepening quenches background η_i-mode turbulence. Although it is not possible to model a global anomalous particle inflow right after gas puffing using the ion-mixing process alone, it should be noted that experimental and modeling results indicate that anomalous particle pinch effects are needed primarily in the near-edge region rather than the central region.[25,26] Thus, ion-mixing turbulence at the edge may be sufficient. Hence, it is possible that improvements in particle confinement after pellet injection are due to a reduction in diffusion rather than an increase in the inward pinch velocity.

2. Impurity effects on particle transport

Recent experimental results from the ISX-B tokamak have indicated that in a neutral beam heated plasma contaminated with small quantities of a recycling low-Z impurity, it is possible to produce a Z-mode discharge[27] characterized by confinement properties which are improved in comparison to the L-mode discharge. The improved energy confinement is accompanied by and thought to be due to peaking of the density profile in the (energy) confinement zone. The global energy confinement time scaling is modified from "ISX-B scaling"[28,29] by introduction of a density dependence. Although transport analyses indicate improved particle confinement in Z-mode discharges, power balance shows that the improved energy confinement is due primarily to a reduction in electron thermal diffusivity χ_e.

In order to explain the improved energy confinement in Z-mode discharge, an extension of the Carreras–Diamond electron thermal diffusivity[30,31] based on resistive ballooning turbulence, has been proposed for the regime where $\omega_{*e} > \gamma$, the linear growth rate. The effect of large ω_* is to reduce the electron thermal diffusivity through diamagnetic modifications to the resistive ballooning mode. The χ_e prediction compares favorably with experimental results.[32] However, even though the proposed large ω_* extension of the Carreras–Diamond χ_e is consistent with experimental results, it is also necessary to explain the improvement of particle confinement and the resulting steepening of the density gradient associated with the introduction of a recycling impurity into the Z-mode discharge.

Here, we propose a mechanism of an ion-mixing driven inward particle flow enhanced by an inverted edge impurity density profile due to (sustained) impurity puffing during Z mode operation. The model of the L to Z phase transition sequence can thus be described as follows.

(i) For the near-edge region of a beam-heated, density-clamped plasma (characteristic of L-mode discharges), the η_i-mode can be destabilized by background ion-temperature-gradient free energy.

(ii) With the introduction of a small amount of low-Z impurity by puffing, background η_i-mode turbulence is amplified by the inverted impurity density profile, providing larger effective η_i values.

(iii) This impurity enhancement effect changes the saturation amplitude of the background η_i-mode turbulence, hence the ion-mixing driven inflow increases and the resulting ambient density profile steepens.

(iv) With the steepening of the density profile, the background resistive ballooning turbulence enters the $\omega_* > \gamma$ regime, which results in a reduced electron thermal diffusivity.

To describe the impurity effects on the η_i-mode,[33] equations for cold impurity ions are necessary. For simplicity, we assume that only one impurity species with charge Z and density n_I is present, and that the concentration of this impurity is small compared to that of background ions, i.e., $Zn_I \ll n_i \lesssim n_e$. For a long-wavelength η_i mode with cold impurity ions (corresponding to the phase velocity regime $v_{\text{th},I} \ll v_{\text{th},i} \lesssim |\omega/k_\parallel| < v_{\text{th},e}$), impurity dynamics equations[13,34] can be derived using equations for impurity ion density and parallel momentum, along with the quasineutrality condition

$$\tilde{n}_e = \tilde{n}_i + Z\tilde{n}_I.$$

Details of the equations are given in Appendix B.

As in the case of the η_i mode, the energy flow and balance can be seen clearly by defining energy-like integrals

$$E^W \equiv \frac{1}{2}\int d^3x\left(|\tilde{\phi}|^2 + \frac{n_{0i}}{n_{0e}}|\nabla_\perp\tilde{\phi}|^2\right), \tag{107}$$

$$E^K \equiv \frac{1}{2}\int d^3x\left(\frac{n_{0i}}{n_{0e}}|\tilde{v}_{\parallel i}|^2\right), \tag{108}$$

$$E^Z \equiv \frac{1}{2}\int d^3x\left(\frac{n_{0I}}{n_{0e}}\frac{m_I}{m_i}|\tilde{v}_{\parallel I}|^2\right), \tag{109}$$

$$E^I \equiv \frac{1}{2}\frac{1}{\Gamma}\int d^3x\left(\frac{n_{0i}}{n_{0e}}|\tilde{p}_i|^2\right). \tag{110}$$

Using the impurity equations, Eqs. (B1)–(B4), it follows that the total energy of the system evolves according to

$$\begin{aligned}\frac{\partial}{\partial t}E &= \frac{\partial}{\partial t}(E^W + E^K + E^Z + E^I)\\ &= -\int d^3x\left[\frac{1}{\Gamma}\left(\frac{1+\eta_i}{\tau}\right)\frac{n_{0i}}{n_{0e}}\frac{1}{L_{ni}}\langle\tilde{p}_i\nabla_y\tilde{\phi}\rangle\right.\\ &\quad\left. - \frac{n_{0i}}{n_{0e}}\mu_i|\nabla_\parallel\tilde{v}_{\parallel i}|^2 - \frac{n_{0I}}{n_{0e}}\frac{m_I}{m_i}\mu_I|\nabla_\parallel\tilde{v}_{\parallel I}|^2\right].\end{aligned} \tag{111}$$

This shows that the structure of the energy balance is the same as in the η_i-mode case, except for an additional sink due to impurity ions. However, μ_I for cold impurity ions is negligible. As described in Sec. III, the required diffusion and radial correlation length at saturation can be estimated and are given by

$$D^I_{\mathbf{k}} \simeq [C(\mathrm{Re})]^2(1+\eta_i/\tau)^{1/2}\frac{k_y}{L_s}(\Delta^I_x)^3\Lambda^{1/2}, \tag{112}$$

$$\Delta^I_{\mathbf{k}} \simeq [D^I_{\mathbf{k}}/k'_\parallel]^{1/4}, \tag{113}$$

respectively, where the additional multiplier of Eq. (85) is included as $C(\mathrm{Re})$, and the enhancement factor is defined by

$$\Lambda \equiv [1 + Z(n_{0I}/n_{0i})\,(L_{ni}/L_{nI})]^{-1}. \tag{114}$$

Here, we assume an inverted impurity density gradient, i.e., $L_{ni}L_{nI} < 0$, and $|Z(n_{0I}/n_{0i})\,(L_{ni}/L_{nI})| < 1$. Basically, the ion-temperature gradient drives fluctuations, and ion parallel viscous dissipation sinks the fluctuation energy, but impurity ions with an inverted density profile effectively enhance η_i, thus amplifying the resulting fluctuations. Similarly, impurity distributions peaked in the center effectively reduce η_i, resulting in lower fluctuation levels and less transport. The most important aspect of this enhancement effect is manifested in the inward particle pinch velocity. With average pinch velocity for the ion-mixing case Eq. (102), the impurity-enhanced pinch velocity can be estimated by

$$\langle V_r\rangle^I \simeq \langle V_r\rangle\cdot\Lambda^3. \tag{115}$$

This enhanced pinch velocity for the edge region of the Z-mode discharge may be responsible for the observed steepening of the density profile after impurity puffing.

V. CONCLUSIONS

For high density regimes of tokamaks in the Ohmic "saturated" phase and in the presence of auxiliary ion heating such as neutral beam injection, significant anomalous energy loss through the ion conduction channel has been observed. Since the ion-temperature gradient is frequently steeper than the density gradient for such regimes of tokamak operation, ion-temperature-gradient-driven turbulence is a strong candidate for the explanation of anomalous ion heat loss in tokamak experiments. Here we have studied ion-temperature-gradient-driven turbulence using two-point equations for the energy correlation function and have calculated the wavenumber spectra of the ion pressure fluctuations. In the saturated state, we have obtained the stationary spectrum from the steady-state solution of the two-point energy correlation equation. Hence, we have calculated fluctuation levels and the resulting ion thermal diffusivity using the spectra. These analytical predictions have been compared with the observed ion thermal diffusivity in the Alcator-C tokamak and are in good agreement.

The principal results of this paper are as follows.

(i) The fluctuation energy correlation function and fluctuation wavenumber spectra are calculated by solution of energy-conserving mode-coupling equations. The calculated wavenumber spectron of ion pressure fluctuations has the form $\langle \tilde{P}_i^2 \rangle_{k_\theta} \sim k_\theta^{-5/2}$, where $(\tilde{P}_i/P_{0i})_{\rm rms} \simeq 5.7[(1+\eta_i)/\tau]^{3/2}\rho_s/L_n$. Similarly, the rms fluctuating radial velocity is

$$(\tilde{v}_r)_{\rm rms} \simeq 2.3[(1+\eta_i)/\tau]^{3/2}\rho_s c_s/L_s$$

and fluctuating density is

$$(\tilde{n}/n_0) = (e\Phi/T_e) \simeq 5.7[(1+\eta_i)/\tau]^{3/2}\rho_s/L_s.$$

Note that the predicted density fluctuation levels are quite similar to the usual drift-wave turbulence level $\tilde{n}/n_0 \approx 3\rho_s/L_n$. Hence, it may be difficult to experimentally distinguish η_i-mode induced density fluctuations from more commonplace low-frequency, drift-wave turbulence unless propagation direction (i.e., ion versus electron) can be resolved. While the parameter scalings of these results are qualitatively consistent with mixing-length estimates, they have been derived using the calculated fluctuation spectra. In particular, no assumptions such as $k_y\rho_s \sim \mathcal{O}(1)$, etc. were used to obtain the numerical coefficients.

(ii) For $\eta_i > \eta_{ic}$, the ion thermal diffusivity χ_i is given by

$$\chi_i = [C(\mathrm{Re})]^2[(1+\eta_i/\tau]^2(k_{0y}\rho_s)(\rho_s^2 c_s/L_s),$$

where $C(\mathrm{Re}) \simeq (\pi/2)\ln(1+\eta_i)$. The numerical value of the ion thermal diffusivity is consistent with the experimentally measured χ_i for the Alcator-C tokamak (for which $k_{0y}\rho_s \simeq 0.4$). Furthermore, for Alcator-C parameters $|C(\mathrm{Re})|^2 \cong 5$, which indicates the importance of the two-point theory in deriving quantitative predictions for comparison with experiment.

(iii) For dissipative trapped electron dynamics (i.e., $\nu_* < 1$, $\nu_{\rm eff} > \bar{\omega}_{De}$), the electron heat conductivity due to ion-temperature-gradient-driven turbulence is given by

$$\chi_e \simeq 15\sqrt{2}\epsilon^{3/2}\left(\frac{\pi}{2}\ln(1+\eta_i)\right)^4\left(\frac{1+\eta_i}{\tau}\right)^3 \frac{c_s^2\rho_s^2}{\nu_e L_s^2}(k_{0y}^2\rho_s^2).$$

Here ϵ is the inverse aspect ratio. Note that in general, $\chi_e \neq \chi_i$ and that χ_e is not determined by considerations of profile consistency.

(iv) For collisional electron dynamics (i.e., $k_\parallel v_{{\rm th},e} < \nu_{ei}$), the electron response to the ion-temperature-gradient-driven turbulence results in a particle flux

$$\Gamma_r \simeq 2n_0[C(\mathrm{Re})]^4[\hat{\chi}_e + (1+\alpha_T)^2] \times\left(1-\frac{\eta_e}{\eta_e^c}\right)\left(\frac{m_e}{m_i}\right)\frac{0.51}{\hat{\chi}_e}\frac{\nu_e}{L_n}\left(\frac{1+\eta_i}{\tau}\right)^2\rho_s^2,$$

where

$$\eta_e^c \simeq \left(\frac{\hat{\chi}_e + (1+\alpha_T)^2}{\frac{3}{2}(1+\alpha_T)}\right) \simeq 1.77.$$

Note that for $\eta_e > 1.77$, the flux is inward. For Alcator-C parameter, $\langle V_r \rangle = \Gamma_r/n_0 \simeq 1000$ cm/sec. Similarly, the electron thermal flux Q_r^e can be derived. For $\eta_e > 2.65$, the electron thermal flux is inward and corresponds to a heat pinch. However, for *collisionless* electron dynamics, the particle flux is always outward. In particular, for $\nu_* < 1$,

$$\Gamma_r \cong \eta_0\epsilon^{3/2}\left(\frac{\omega_{*e}(1+\frac{3}{2}\eta_e) - \mathrm{Re}(\omega)}{\nu_{ei}}\right) \times\left(\frac{\pi^2}{4}[\ln(1+\eta_i)]^2\right)^2\left(\frac{1+\eta_i}{\tau}\right)^3\frac{(k_y\rho_s)_{\rm rms}\rho_s^2 c_s}{L_s^2}.$$

Hence, Γ_r *decreases* with η_i, thus reconciling energy and particle confinement time behavior during pellet injection experiments.

(v) The effects of impurity gradients of ion-temperature-gradient-driven turbulence have been investigated. For impurity density n_{0I} with scale length L_{nI}, $\chi_i \to \chi_i\Lambda^2$ and $\Gamma_r \to \Gamma^r\Lambda^3$, where $\Lambda = [1 + Z(n_{0I}/n_{0i})(L_{ni}/L_{nI})]^{-1}$. Thus impurity distributions peaked on axis heal η_i-mode turbulence while distributions peaked at the edge enhance it. In particular, the enhancement of Γ_r may underlie the density profile steepening observed during the Z mode of the ISX-B tokamak.

In this paper, a sheared slab model of ion-temperature-gradient-drive turbulence was used in order to elucidate the basic physics and phenomenological consequences in a simple and clear fashion. Although little change in the basic conclusions is to be expected, the theory can be applied to the toroidal branch of the η_i mode using the large-n ballooning representation. This will be discussed in a future publication.

ACKNOWLEDGMENTS

The authors would like to thank Professor B. Coppi, Professor M. N. Rosenbluth, and Dr. W. M. Tang for their interest, encouragement and useful conversations. We are grateful to Dr. P. Terry and Dr. T. S. Hahm for a careful reading of the manuscript. Finally, helpful discussions of experimental results with Dr. D. W. Ross, Dr. W. I. Rowan, Dr. A. J. Wootton, Dr. S. Wolfe, Dr. M. Greenwald, Dr. G. Becker, and Dr. F. Wagner are also acknowledged.

This research was supported by the United States Department of Energy under Contract No. DE-FG05-80ET-53088.

APPENDIX A: THE FOURIER TRANSFORM OF THE RADIALLY AVERAGED CORRELATION LIFETIME

Here, we provide the details of the derivation of Eq. (83),

$$F(k_y k_z) = -\frac{1}{\Delta_x}\int_0^{\Delta_x} dx_- \int dy_- \int dz_-\, e^{-ik_y y_- - ik_z z_-}\, \bar{\tau}_{cl}(x_-,y_-,z_-)$$

$$= -\frac{1}{\Delta_x}\int_0^{\Delta_x} dx_- \int dy_- \int dz_-\, e^{-k_y y_- - ik_z z_-} \ln\left[\left(\frac{\alpha}{\alpha+1}\right) + C\left[(1+\alpha)k_{0x}^2 x_-^2 + k_{0y}^2 y_-^2 + k_{0z}^2 z_-^2\right]\right]. \tag{A1}$$

Transforming to a polar coordinate system given by

$$u^2 = [x_-^2/\Delta_x^2], \quad \rho^2 = C(k_{0y}^2 y_-^2 + k_{0z}^2 z_-^2), \quad y_- = (\rho/k_{0y}\sqrt{C})\sin\theta, \quad z_- = (\rho/k_{0z}\sqrt{C})\cos\theta, \tag{A2}$$

this yields

$$F(k_y,k_z) = \left(\frac{2}{k_{0y}k_{0z}C}\right)\int_0^{\sqrt{1-\alpha^2}} \rho\, d\rho \int_0^{2\pi} d\theta \exp\left\{-i\left[\frac{\rho}{\sqrt{C}}\left(\frac{k_y}{k_{0y}}\sin\theta + \frac{k_z}{k_{0z}}\cos\theta\right)\right]\right\}$$

$$\times\left[\sqrt{1-(\alpha^2+\rho^2)} - \sqrt{\alpha^2+\rho^2}\cos^{-1}(\sqrt{\alpha^2+\rho^2})\right], \tag{A3}$$

where $\alpha^2 \equiv \alpha/(\alpha+1)$. Using Jacobi–Anger expansion,[35] i.e.,

$$\int_0^{2\pi} d\theta \exp\left(-ip\left\{\sqrt{C}\left[\left(\frac{k_y}{k_{0y}}\right)\sin\theta + \left(\frac{k_z}{k_{0z}}\right)\cos\theta\right]\right\}^{-1}\right) = \sum_{m=-\infty}^{\infty} (-i)^m (2\pi) J_m\left(\frac{k_y\rho}{k_{0y}\sqrt{C}}\right) J_m\left(\frac{k_z\rho}{k_{0z}\sqrt{C}}\right), \tag{A4}$$

and using Neumann's addition theorem for Bessel functions, i.e.,

$$J_0\left(\frac{\beta}{\sqrt{C}}\rho\right) = \sum_{m=-\infty}^{\infty} (-i)^m J_m\left(\frac{k_y}{k_{0y}\sqrt{C}}\rho\right) J_m\left(\frac{k_z}{k_{0z}\sqrt{C}}\rho\right), \tag{A5}$$

where $\beta = \sqrt{(k_y/k_{0y})^2 + (k_z/k_{0z})^2}$, we then arrive at the expression given in Eq. (83),

$$F(k_y,k_z) = \left(\frac{4\pi}{Ck_{0y}k_{0z}}\right)\int_0^{\sqrt{1-\alpha^2}} \rho\, d\rho\, J_0\left(\frac{\beta}{\sqrt{C}}\rho\right)\left[\sqrt{1-(\alpha^2+\rho^2)} - \sqrt{\alpha^2+\rho^2}\cos^{-1}(\sqrt{a^2+\rho^2})\right]. \tag{A6}$$

For the large Reynolds number regime, Eq. (A6) can be approximated by

$$F(k_y,k_z) = \left(\frac{4\pi}{k_{0y},k_{0z}}\right)\int_0^1 \rho\, d\rho\, J_0(\beta\rho)\left[\sqrt{1-\rho^2} - \rho\cos^{-1}\rho\right]. \tag{A7}$$

Integrating over k_z yields the polodial wavenumber spectrum given in Eq. (84)

$$F(k_y) = \left(\frac{4\pi^2}{k_{0y}}\right)\left(\frac{k_{0y}}{k_y}\right)^2\left[1 - J_0\left(\frac{k_y}{k_{0y}}\right)\right]. \tag{A8}$$

APPENDIX B: FLUID EQUATIONS FOR IMPURITY GRADIENT EFFECTS

We outline the derivation of model equations of impurity gradient effects η_i-mode turbulence discussed in Sec. IV B. The fluid model consists of equations for background ions, Eqs. (2)–(5), and equations for cold impurity ions. Using the same normalization as in Sec. II and the quasineutrality condition gives

$$\frac{\partial}{\partial t}\left(1 - \frac{n_{0i}}{n_{0e}}\nabla_\perp^2\right)\tilde{\phi} + \frac{1}{n_{0e}}\left(\frac{n_{0i}}{L_{ni}} + \frac{Zn_{0I}}{L_{nI}}\right)\nabla_y\tilde{\phi} + \left(\frac{1+\eta_i}{\tau}\right)$$

$$\times\frac{\eta_{0i}}{n_{0e}}\frac{1}{L_{ni}}\nabla_y(\nabla_\perp^2\tilde{\phi}) - \frac{n_{0i}}{n_{0e}}\hat{b}\times\nabla\tilde{\phi}\cdot\nabla_\perp(\nabla_\perp^2\tilde{\phi})$$

$$+\frac{n_{0i}}{n_{0e}}\nabla_\parallel\tilde{v}_{\parallel i} + Z\frac{n_{0I}}{n_{0e}}\nabla_\parallel\tilde{v}_{\parallel}I = 0, \tag{B1}$$

$$\frac{\partial}{\partial t}\tilde{v}_{\parallel i} + \hat{b}\times\nabla\tilde{\phi}\cdot\nabla\tilde{v}_{\parallel i} - \mu_i\nabla_\parallel^2\tilde{v}_{\parallel i} = -\nabla_\parallel\tilde{\phi} - \nabla_\parallel\tilde{p}_i, \tag{B2}$$

$$\frac{\partial}{\partial t}\tilde{v}_{\parallel I} + \hat{b}\times\nabla\tilde{\phi}\cdot\nabla\tilde{v}_{\parallel I} - \mu_I\nabla_\parallel^2\tilde{v}_{\parallel I} = -Z\frac{m_i}{m_I}\nabla_\parallel\tilde{\phi}, \tag{B3}$$

$$\frac{\partial}{\partial t}\tilde{p}_i + \hat{b}\times\nabla\tilde{\phi}\cdot\nabla\tilde{p}_i + \left(\frac{1+\eta_i}{\tau}\right)\frac{1}{L_{ni}}\nabla_y\tilde{\phi} = -\frac{\Gamma}{\tau}\nabla_\parallel\tilde{v}_{\parallel i}, \tag{B4}$$

where n_{0i}, n_{0e}, and n_{0I} are background ion density, electron density, and impurity density, respectively.

[1] M. Greenwald, D. Gwinn, S. Milora, J. Parker, R. Parker, and S. Wolfe, *10th International Conference on Plasma Physics and Controlled Nuclear Fusion Research*, London (IAEA, Vienna, 1984), Vol. I, p.45.
[2] S. M. Wolfe and M. Greenwald, Nucl. Fusion **26**, 329 (1986).
[3] R. J. Groebner, W. W. Pfeiffer, F. P. Blau, and K. H. Burrell, Nucl. Fusion **26**, 543 (1986).
[4] B. Coppi, M. N. Rosenbluth, and R. Z. Sagdeev, Phys. Fluids **10**, 582 (1967); L. I. Rudakov and R. Z. Sagdeev, Dokl. Akad. Nauk. SSSR **138**, 581 (1961) [Sov. Phys. Dokl. **6**, 415 (1965)].
[5] B. Coppi and C. Spight, Phys. Rev. Lett. **41**, 551 (1978).
[6] L. Garcia, P. H. Diamond, B. A. Carreras, and J. D. Callen, Phys. Fluids **28**, 2137 (1985).

[7]T. Antonsen, B. Coppi, and R. Englade, Nucl. Fusion **19**, 641 (1979).
[8]W. Horton, D-I. Choi, and W. M. Tang, Phys. Fluids **24**, 1077 (1981).
[9]W. Horton, R. D. Estes, and D. Biskamp, Plasma Phys. **22**, 663 (1980).
[10]G. S. Lee and P. H. Diamond, *Proceedings of Annual Controlled Fusion Theory Conference* (University of Wisconsin, Madison, 1985), p. 1S24.
[11]J. W. Connor, Nucl. Fusion **26**, 193 (1986); J. W. Connor and J. B. Taylor, Phys. Fluids **27**, 2676 (1984).
[12]P. N. Guzdar, Liu Chen, W. M. Tang, and P. H. Rutherford, Phys. Fluids **26**, 673 (1983).
[13]S. I. Braginskii, in *Review of Plasma Physics*, edited by M. A. Leontovich (Consultants Bureau, New York, 1965), Vol. I, p. 205.
[14]F. L. Hinton and C. W. Horton, Phys. Fluids **14**, 116 (1971).
[15]Y. K. Pu and S. Migliuolo, Phys. Fluids **28**, 1722 (1985); S. Migliuolo, Phys. Fluids **28**, 2778 (1985).
[16]R. E. Waltz, W. Pfeiffer, and R. R. Dominguez, Nucl. Fusion **20**, 43 (1980).
[17]P. H. Diamond, R. D. Hazeltine, Z. G. An, B. A. Carreras, and H. R. Hicks, Phys. Fluids **27**, 1449 (1984).
[18]P. W. Terry and P. H. Diamond, Phys. Fluids **28**, 1419 (1985).
[19]A. Hasegawa and K. Mima, Phys. Rev. Lett. **39**, 205 (1977).
[20]T. H. Dupree, Phys. Fluids **15**, 334 (1972).
[21]C. S. Chang and F. L. Hinton, Phys. Fluids **25**, 1493 (1982).
[22]G. Becker, *12th European Conference on Controlled Fusion and Plasma Physics*, Budapest (EPS, Budapest, 1985), Vol. II, p. 454.
[23]Z. G. An, G. S. Lee, and P. H. Diamond, submitted to Phys. Fluids.
[24]J. C. Adam, W. M. Tang, and P. H. Rutherford, Phys. Fluids **19**, 561 (1976).
[25]Yu. N. Dnestrovskii, S. V. Neudachin, and G. V. Pereverzev, Fiz. Plazmy **10**, 236 (1984) [Sov. J. Plasma Phys. **10**, 137 (1984)].
[26]D. W. Ross and W. L. Rowan (private communication, 1985).
[27]E. A. Lazarus, J. Nucl. Mater. **121**, 61 (1984).
[28]G. H. Neilson, E. A. Lazarus, M. Murakami, A. J. Wootton, and J. L. Dunlap, Nucl. Fusion **23**, 285 (1983).
[29]D. W. Swain and G. H. Neilson, Nucl. Fusion **22**, 1015 (1982).
[30]B. A. Carreras, P. H. Diamond, and M. Murakami, Phys. Rev. Lett. **50**, 503 (1983).
[31]P. H. Diamond, P. L. Similon, T. C. Hender, and B. A. Carreras, Phys. Fluids **28**, 1116 (1985).
[32]M. Murakami, P. H. Edmonds, and G. A. Hallock, *10th International Conference on Plasma Physics and Controlled Nuclear Fusion Research*, London (IAEA, Vienna, 1984), Vol, I, p. 87.
[33]B. Coppi, H. P. Furth, M. N. Rosenbluth, and R. Z. Sagdeev, Phys. Rev. Lett. **17**, 377 (1966).
[34]W. M. Tang, R. B. White, and P. N. Guzdar, Phys. Fluids **33**, 167 (1980).
[35]G. N. Watson, *A Treatise on the Theory of Bessel Functions* (Cambridge U. P., Cambridge, 1966).